Involvement of PKCzeta, GSK3beta, and MAPK in maintenance of the mitotic spindle

by

Madhavi Chakravadhanula

A Dissertation Presented in Partial Fulfillment
of the Requirements for the Degree
Doctor of Philosophy

Approved November 2012 by the
Graduate Supervisory Committee:

David Capco, Chair
Douglas Chandler
Josephine Clark-Curtiss
Stuart Newfeld

ARIZONA STATE UNIVERSITY

December 2012

ABSTRACT

In somatic cells, the mitotic spindle apparatus is centrosomal and several isoforms of Protein Kinase C (PKC) have been associated with the mitotic spindle, but their role in stabilizing the mitotic spindle is unclear. Other protein kinases such as, Glycogen Synthase Kinase 3β (GSK3β) also have been shown to be associated with the mitotic spindle. In the study in chapter 2, we show the enrichment of active (phosphorylated) PKCζ at the centrosomal region of the spindle apparatus in metaphase stage of 3T3 cells. In order to understand whether the two kinases, PKC and GSK3β are associated with the mitotic spindle, first, the co-localization and close molecular proximity of PKC isoforms with GSK3β was studied in metaphase cells. Second, the involvement of inactive GSK3β in maintaining an intact mitotic spindle was shown. Third, this study showed that addition of a phospho-PKCζ specific inhibitor to cells can disrupt the mitotic spindle microtubules. The mitotic spindle at metaphase in mouse fibroblasts appears to be maintained by PKCζ acting through GSK3β. The MAPK pathway has been implicated in various functions related to cell cycle regulation. MAPKK (MEK) is part of this pathway and the extracellular regulated kinase (ERK) is its known downstream target. GSK3β and PKCζ also have been implicated in cell cycle regulation. In the study in chapter 3, we tested the effects of inhibiting MEK on the activities of ERK, GSK3β, PKCζ, and α-tubulin. Results from this study indicate that inhibition of MEK did not inhibit GSK3β and PKCζ enrichment at the centrosomes. However, the mitotic spindle showed a reduction in the pixel intensity of microtubules and also a reduction in the number of cells

in each of the M-phase stages. A peptide activation inhibitor of ERK was also used. Our results indicated a decrease in mitotic spindle microtubules and an absence of cells in most of the M-phase stages. GSK3β and PKCζ enrichment were however not inhibited at the centrosomes. Taken together, the kinases GSK3β and PKCζ may not function as a part of the MAPK pathway to regulate the mitotic spindle.

DEDICATION

To all my family especially my parents, my husband, and my kids for all their support throughout the period of my doctoral studies. This doctoral work would not be possible without their unfailing support and help.

ACKNOWLEDGMENTS

I wish to thank my mentor and doctoral committee chair, Dr. David Capco for being very patient with me and guiding me through the doctoral program. Dr. Capco taught me some important lessons in the scientific method, scientific writing, scientific presentation, and very important lessons for a good scientific career in the future. I wish to thank Dr. Stuart Newfeld for his very valuable and timely advice as a member of my doctoral committee. I thank Dr. Josephine Clark-Curtiss and Dr. Doug Chandler for all their valuable suggestions and advice as members of my doctoral committee. I thank Dr. Page Baluch, manager of the Keck bio-imaging facility at ASU, for her help with my work that involved microscopic imaging. I thank David Lowry, manager of the electron microscopy facility at ASU, for his help with my electron microscopy work. I thank Dr. Scott Bingham, associate research scientist and manager of the molecular biology core facility at ASU for his guidance with my molecular biology work. I thank Dr. Brian Koeneman, James Faust, and Anup Abraham for their help in the laboratory. I thank Rick Olsen, Wendi Simonson, and Yvonne Delgado for all their help.

TABLE OF CONTENTS

Page

LIST OF FIGURES vii

CHAPTER

1 INTRODUCTION 1

2 INVOLVEMENT OF PKC ZETA AND GSK3 BETA IN THE STABILITY OF THE METAPHASE SPINDLE 20

Introduction 20

Materials and Methods 22

Results 30

Discussion 48

3 INVOLVEMENT OF MEK, ERK, PKC ZETA AND GSK3 BETA IN MAINTAINING THE MITOTIC SPINDLE 55

Introduction 55

Materials and Methods 59

Results 65

Discussion 87

4 CONCLUDING THOUGHTS 92

Conclusions from Chapter 2 92

Conclusions from Chapter 3 93

Future Studies 95

REFERENCES 98

LIST OF FIGURES

Figure Page

1. Assembly of microtubules that are part of the mitotic spindle apparatus 5
2. Domain structure of protein kinase C (PKC) isoforms 7
3. Summary of various reports on the location of the different PKC isotypes at key points in mouse oocyte development 10
4. Alignment of the V5 domain in PKC isoforms..... 13
5. Substrates of GSK3……14
6. An overview of MAPK pathways involved in a signaling network in mammalian cells……....18
7. Enrichment of phospho(p)-PKC isoforms in 3T3 metaphase cells-intact and detergent-extracted (DE)……..32
8. Co-localization of the different phospho isoforms of PKC with p(ser9)GSK3β……...35
9. FRET values measured between pPKCζ or pPKCδ and p(ser9)GSK3β at metaphase stage of 3T3 cells……....37
10. Western analysis of 3T3 cells at metaphase stage to show interaction of pPKC isotypes with p(ser9)GSK3β…….39
11. 3T3 cells permeabilized and treated with active GSK3β kinase…. 42
12. Effect of the inhibition of pPKCζ by a myristoylated pPKCζ peptide-specific inhibitor on α-tubulin and p(ser 9)GSK3β in 3T3 cells…..45
13. Western analysis of 3T3 cells treated with pPKCζ inhibitor and

Figure Page

immunopurified to test the effects of the inhibitor on p(ser9)GSK3β and pericentrin binding…….47

14. Effect of MEK inhibition on the co-localization of pMEK with p(ser9)GSK3β and pPKCζ in 3T3 cells……68

15. Western analysis of MEK inhibited cell lysates……...71

16. Confirmation of MEK siRNA specificity; Effect of MEK over-expression……75

17. Effect of MEK inhibition on α-tubulin…….79

18. Cell numbers in mitotic stages after MEK inhibition……...82

19. Effects of ERK activation peptide inhibitor……..85

20. Predicted model from the results in Chapter 2 and Chapter 3……..95

Chapter 1

INTRODUCTION

The events that are involved in cell cycle progression are tightly regulated to maintain the viability of the cell and to correctly pass cytoplasm and genetic information to daughter cells. Accurate chromosome segregation during meiosis and mitosis is a requirement that allows cells to faithfully transmit their genetic information to daughter cells. A disruption in the regulation of any of these cell cycle events can lead to cell death and can significantly contribute to malignant transformation (Rao et al. 2009). The accurate seggregation of chromosomes during mitosis and meiosis occurs on a highly ordered macromolecular machine, the spindle apparatus. Assembly of the spindle is a dynamic process and maintenance of the bipolar array of the microtubules requires a constant dissipation of energy (Vernos and Karsenti, 1995). To ensure faithful segregation of chromosomes, microtubules emanating from spindle poles attach to and align chromosomes at the metaphase plate before segregating the sister chromatids evenly between daughter cells. In order to fulfill this aim, kinetochores, or macromolecular protein complexes associated with centromeres, must stably attach to dynamic microtubules (Ricke and Deursen, 2011).

In the mouse egg the meiotic spindle is acentrosomal, in contrast to the mouse fibroblasts where the mitotic spindle is centrosomal. The mouse egg has a natural cell cycle arrest point after the formation of the acentrosomal metaphase II spindle. Studies have shown that spindles formed in the absence of centrioles are

thought to be nucleated at the chromosomes (Caudron et al. 2005; Hertzer, 2006). The microtubules then converge at the spindle poles by means of minus-end molecular motors (Goshima et al., 2005) forming a barrel-shaped structure (Szollosi et al., 1972). In the mammalian egg, after fertilization there is a precise series of signaling events that orchestrate its conversion into a zygote. These signals are precisely regulated and some are mediated through cytoskeletal scaffolds (Capco, 2001; Baluch and Capco, 2002).

In somatic cells including mouse fibroblasts the mitotic spindle is centrosomal where the centrosome is the primary microtubule-organizing center (MTOC). At the heart of each centrosome present in most animal cells there are two centrioles. Centrioles are cylindrically shaped organelles made of nine microtubule (MT) triplets organized in a nine-fold symmetrical configuration. Centrioles are present in many eukaryotes and are essential for the formation of several microtubule-organizing structures including centrosomes and cilia (Debec et al. 2010). The centriole remains a surprisingly mysterious organelle. Although there have been many recent advances in the comprehension of its structure and functions, it remains, a kind of ‘‘terra incognita’’ of the cell (Paoletti and Bornens, 1997; Debec et al. 2010). Many studies have observed that the mitotic spindle apparatus is composed of several elements including centrosomes, microtubules such as astral, polar, and kinetochore microtubules, kinetochores of chromosomes, and associated proteins (McIntosh and Landis, 1971; Burbank et al., 2007; Walczak and Heald, 2008; Schmidt et al., 2010).

The proper attachment and alignment of the chromosomes, which occurs during prometaphase, is the defining aspect of mitosis. During prometaphase, chromosomes exhibit a complex pattern of movement that is often described as "the dance of chromosomes" in classic cytology literature. In this dance, some chromosomes move poleward, while other chromosomes move away from the spindle poles drawn by association with the kinetochore microtubules, and others remain relatively motionless (Walczack et al. 2010). Over time, these seemingly chaotic movements result in the congression of chromosomes to the spindle equator, such that more and more chromosomes become aligned between the separated spindle poles. The key interaction between chromosomes and microtubules occurs at the centromere of the chromosome, which contains macromolecular complexes termed kinetochores. The known structure of a kinetochore consists of an inner plate, a chromatin structure containing nucleosomes with at least one specialized histone, auxiliary proteins and DNA. The makeup and organization of this DNA is not well understood in animal cells. The inner plate exists as a discrete heterochromatin domain throughout the cell cycle (Maiato et. al. 2004). Outside this is an outer plate composed primarily, if not solely, of protein (Cooke et al. 1993). This structure forms on the surface of the chromosome at about the time of nuclear envelope breakdown (Brinkley and Stubblefield, 1966; Ris and Witt, 1981; McEwen et al., 1993). The outer plate of vertebrate kinetochores has about 20 end-on attachment sites for the plus ends of microtubules, termed kinetochore microtubules. Challenges for a cell are, ensuring that the spindle microtubules attach properly to each of the many

chromosomes, positioning them at the spindle equator and ultimately driving the poleward movement of sister chromatids to the opposite poles of the spindle. The segregation of multiple chromosomes in a cell must be executed in perfect synchrony, which implies that the state of every chromosome is monitored by the spindle and that mitotic exit is delayed until all chromosomes are attached. This monitoring is achieved through a pathway termed the spindle assembly checkpoint (Musacchio and Salmon, 2007). Sporadic errors in chromosome attachment to the spindle microtubules are inevitable given the complexity of the system. Failure to correct these errors results in chromosome mis-segregation, and one of the outcomes is aggressive malignancies (Rajagopalan and Lengauer, 2004; Holland and Cleveland, 2009). How the spindle integrates all of its tasks remains unclear. Studies conducted on microtubules during interphase indicate that microtubules are dynamic polymers that are assembled from tubulin heterodimers and these tubulin heterodimers are organized such that the microtubules have an intrinsic polarity (Fig. 1a). Microtubules undergo periods of polymerization and depolymerization and interconvert randomly between these states, a property known as dynamic instability. Although microtubules exhibit dynamic instability at both ends of the microtubule, the plus ends are more dynamic than the minus ends. Microtubules in the spindle also exhibit dynamic instability (Fig. 1b), which occurs primarily at the plus ends of the microtubules as the minus ends are often capped at the centrosome. However, spindle microtubules and kinetochore (k)-fibres exhibit an additional dynamic property, known as microtubule flux, in which there is a net addition of tubulin

heterodimers at the plus ends near the kinetochores and a net loss of tubulin subunits at the minus ends near the centrosomes (Fig. 1c) (Walczak et al. 2010; Zhu et al. 2009).

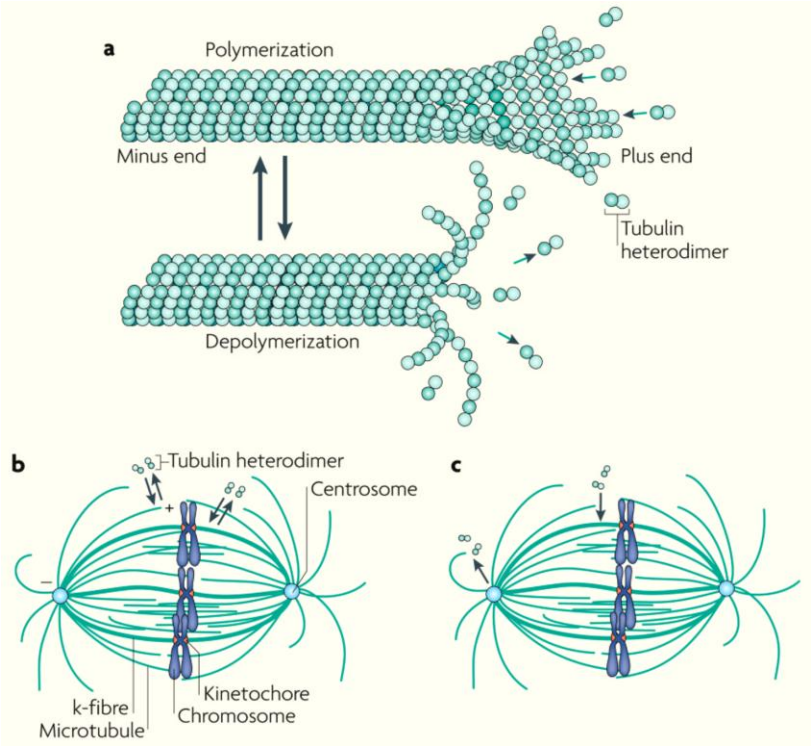

Figure 1: Assembly of microtubules that are part of the mitotic spindle apparatus (Adopted from Walczak et al. 2010).

At the microtubule organizing centers in cells containing centrioles and/or centrosomes, the "plus" ends of microtubules extend from the centrosomal region and are captured and stabilized by the kinetochore (Vernos and Karsenti, 1995; Zhang and Nicklas, 1995; Heald et al. 1996; Brunet et al. 1998; Caudron et al. 2005; Tulu et al. 2006). This type of assembly has been referred to as the "search

and capture model". In contrast, in cells that do not contain centrosomes such as mouse eggs, microtubules emanate from the chromosomes, become associated with molecular motor proteins and are thought to bundle the microtubules to form the bipolar spindle apparatus (Karsenti and Vernos, 2001; Caudron et al. 2005; Goshima et al. 2005; Tulu et al. 2006).

In the meiotic metaphase II (MII) mouse egg, as well as in somatic cells, many signaling elements such as Protein Kinase C (PKC), Calcium/calmodulin dependent protein kinase II (CaM KII) and Mitogen-Activated Protein kinase (MAPK) are found to be enriched at the meiotic and mitotic spindle (Abbott and Ducibella, 2001; Collelo et al. 2012; Hatch and Capco, 2001, Shapiro et al. 1998; Willard and Crouch, 2001).

Protein kinase C (PKC) is one of the important signaling elements involved in meiotic and mitotic events. PKC exists as 11 isotypes, several of which can exist simultaneously in a single cell. Many of the isotypes have different cofactor requirements for activation and function at different sites within the cell when active. Presumably, they act to render differential functionality to various cellular events. There are three broad categories of PKC based on their requirements and the structure of their regulatory domains at the NH2 terminus (Fig. 2). The conventional PKCs namely, PKCα, βI, βII, and γ are diacylglycerol (DAG), phospholipids, and calcium dependent, with their regulatory domains containing a C1 domain which binds DAG/PMA and a C2 domain which binds anionic phospholipids in a calcium dependent manner. The novel PKCs are DAG and phospholipid dependent, but are calcium independent and include PKCδ, ε, μ,

η, and θ; their regulatory domains contain two C1 and one C2 domain with the C2 domains lacking the calcium-coordinating acidic residues. The atypical PKCs are DAG and calcium independent and include PKCζ and human PKCι/mousePKCλ; their regulatory domains lack the calcium-sensitive C2 domain and contain the atypical C1 domain that binds PIP2 or ceramide (Liu et al. 2006).

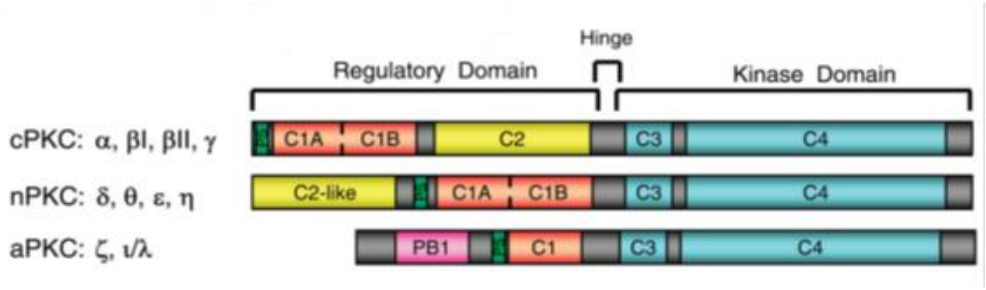

Figure 2: Domain structure of protein kinase C (PKC) isoforms. PKCs have a conserved kinase domain (depicted in teal) and more variable regulatory domains. All PKC regulatory domains have a pseudosubstrate motif (shown in green) NH2 terminal to the C1 domain (shown in pink). Tandem C1 domains are the molecular sensors of phorbol 12-myristate 13-acetate (PMA)/diacylglycerol (DAG) in cPKC and nPKC isoforms, whereas the single aPKC C1 domain does not bind DAG/PMA. The C2 domains (in yellow) function as calcium-dependent phospholipid binding modules in cPKCs. Novel PKC C2 domains do not bind calcium; the PKC*δ*-C2-like domain is a phosphotyrosine interaction module. PKC isoform variable regions are shown in gray (Steinberg, 2008).

Studies conducted in yeast, *Caenorhadbitis elegans*, *Drosophila*, and other cell culture lines discovered that phosphorylated PKCζ (p-PKCζ) plays a role in polarity, microtubule nucleation, and microtubule stability which suggests that PKC has a important role in cytoskeletal regulation (Watts et al. 1996; Joberty et al. 2000; Johansson et al. 2000; Cox et al. 2001; Goold and Gordon-Weeks,

2004a; Etienne-Manneville et al. 2005; Yoshimura et al. 2005). As a result of these studies, elements of the PKCζ signaling pathway have emerged. The wide spectrum of PKC mediated signaling is organized by isoform specificity. The activation and degradation of the PKC isoforms is controlled spatially and temporally, since cells and/or tissues often produce more than one PKC isoform.

PKC isoforms can have broad overlapping substrate specificities, but their unique functionality may be defined via unique expression patterns, intracellular localization, and adaptor proteins (Meier et al. 2009). Some of the substrates that PKC isoforms act on are: MARCKS proteins, RACK proteins, Dynamin, Vinculin, EGFR, and MEK5 (Steinberg, 2008; Meier et al. 2009). Earlier studies have shown that mouse eggs arrested at metaphase II contain PKCα, γ, δ, and ζ (Pauken and Capco, 2000; Baluch et al. 2004) at specific locations (Fig. 3). In oocytes, the nuclear envelope is disassembled at the onset of M-phase, perhaps in part by the action of PKC (Wilding et al. 1996), the interphase array of microtubules is disassembled as well and replaced during meiosis by the meiotic spindle. Even in the absence of the nuclear envelope, different substrate specificities of enzymes can continue to contribute to each enzyme acting at a specific location (Fig. 3). One such study (Avazeri et al., 2004) shows that PKCα, βI, βII, and γ are initially absent from the germinal vesicle, but later, prior to germinal vesicle breakdown, PKCα, βI, and βII enter the nucleus (Fig. 3). Other studies that examined only one isotype of PKC confirm the presence of PKCα (Quan et al. 2003) and PKCβI (Denys et al. 2007) in the nucleus prior to germinal vesicle disruption. One study examined PKCα, βI, and βII and found all three in

the cytoplasm of germinal vesicle stage oocytes (Luria et al. 2000) which is in agreement with the studies above at an early germinal vesicle stage (Avazeri et al. 2004). The main focus of that study was to apply PMA as an agonist to activate PKCs (Luria et al. 2000). This treatment caused resumption of the meiotic cell cycle with the consequent disruption of the germinal vesicle. PKCδ has been identified in the oocyte germinal vesicle as well as the cytoplasm at a time when biochemical analysis demonstrates that PKC activity is elevated (Fig. 3). Later PKCδ was shown to associate with the spindle apparatus in meiosis I (Viveiros et al. 2001, 2003), and that the active form of PKCδ (i.e., p-PKCδ) was specifically enriched at the spindle poles where it was co-localized with pericentrin and γ-tubulin (Ma et al. 2008). The fertilization-competent metaphase II stage egg exhibits notable differences in the position of several isotypes of PKC (Fig. 3). Antibodies that detect both unphosphorylated forms and phosphorylated forms of each isotype, hereafter referred to as ‘‘total’’ PKC, were present at a lower level in the cytoplasm, but enriched on the spindle apparatus for total PKCα, γ, δ, and ζ (Baluch et al. 2004). Total PKCζ remained behind after the detergent extraction, and this was further confirmed by FRET analysis between α-tubulin and the PKC isotypes. FRET revealed a close molecular association only between α-tubulin and PKCζ and between a-tubulin and PKCδ (Baluch et al. 2004; Baluch and Capco, 2008).

Other investigators have shown that PKCβ is present in the egg cytoplasm (Raz et al. 1998). In eggs, pPKCζ is enriched at the ends of the acentrosomal spindle, whereas total PKCζ is attached along the length of the

spindle apparatus. It has been suggested that PKCζ has a role in the asymmetric positioning of the spindle apparatus in mouse eggs (Na and Zernicka-Goetz, 2006). Some evidence exists to suggest a role for pPKCδ in spindle stability (Ma et al. 2008) as pPKCδ is enriched at the spindle poles in the same areas as pPKCζ in the metaphase egg. A targeted knockdown of PKCδ expression with siRNA disrupts the spindle. This same knockdown experiment also decreased expression of pericentrin, thus the knockdown may have several effects on the egg's spindle apparatus (Ma et al. 2008). The reduction in pericentrin would provide no place for pPKCδ to bind at the poles and may have even decreased the concentration of pPKCζ at the poles. Either of these results would be expected to disrupt the spindle since pPKCζ activity is required for spindle stability as described earlier (Baluch et al. 2004). In mouse oocytes, when free-calcium levels are low, calcium-independent kinases such as PKCζ may regulate the stability of the meiotic spindle (Baluch and Capco, 2008).

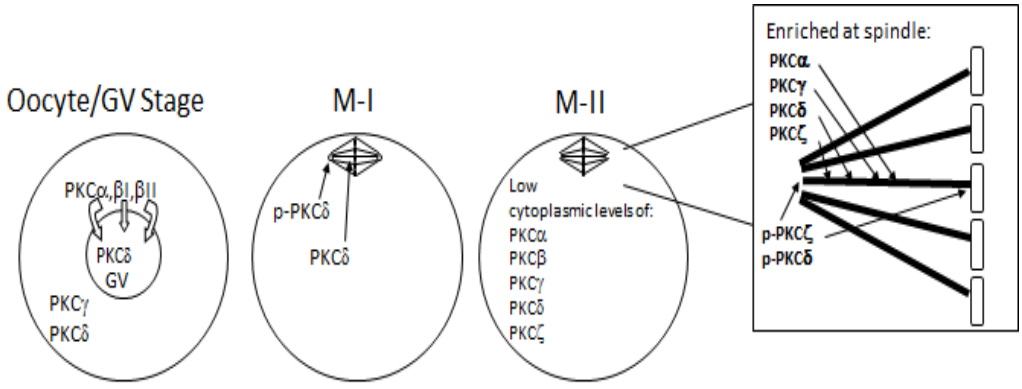

Figure 3: Summary of various reports on the location of the different PKC isoforms at key points in mouse oocyte development. In these diagrams p-PKC represents phosphorylated forms of the kinase while PKC represents both the phosphorylated and nonphosphorylated forms of the kinase (Kalive et al. 2010).

Some of the PKC isoforms in somatic cells with a centrosomal mitotic spindle, have been shown to be associated with the microtubules or the centrosome of the spindle apparatus, although their role in spindle stability has not been elucidated. These include PKC βI, βII, ε, θ, δ, and ζ (Lehrich and Forrest, 1994; Kiley and Parker, 1995; Volkov et al. 1998; Passalacqua et al. 1999). The attachment of spindle microtubules to kinetochores is crucial for accurate segregation of chromosomes to daughter cells during mitosis. PKCζ was shown to be localized at the mitotic spindle during mitosis and to play a role in stable kinetochore-microtubule attachment. In this study, treatment of cells with the PKCζ inhibitor dislocated the minus-end directed motor protein dynein from kinetochores, but did not affect the mitotic checkpoint proteins Mad2 and CENP-E and prolonged exposure to the PKCζ inhibitor eventually resulted in cell death. These results suggest a critical role of PKCζ in spindle microtubule-kinetochore attachment and subsequent chromosomal separation (Liu et al. 2006). Location is a critical determinant in dictating the cellular function of PKC. Scaffold proteins contribute to localization by poising PKC at specific intracellular sites. An earlier study identified the centrosomal protein pericentrin as a scaffold that tethers PKC βII to centrosomes. Disruption of this interaction results in release of PKC from the centrosome, microtubule disorganization, and cytokinesis failure, indicating a specific regulatory role of this isozyme in centrosome function (Chen et al. 2004). PKCε was shown to be anchored at the Golgi/centrosome area by, centrosome and Golgi localized PKN- associated protein (CG-NAP) after being

hypophosphorylated. CG-NAP serves as a scaffold for the phosphorylation reaction of PKCε (Takahashi, 2000).

In the PKC isoforms, V5 domains play an important role in orchestrating isoform specific functions. V5 domains (Fig. 4) are 50- to 70-amino acid sequences that contain highly conserved turn and hydrophobic phosphorylation motifs as well as, additional 7–21 residues at the extreme COOH terminus (beyond the hydrophobic motif) that are highly variable both in their length and sequence. The extreme COOH-terminal regions of the V5 domain that share little to no sequence homology have been exploited as epitopes to raise PKC isoform-specific antibodies for Western blotting and immuno-localization studies. These regions were otherwise generally ignored in early studies exploring the structural determinants of PKC isoform function. However, V5 domains have recently emerged as structures that impart important determinants of PKC isoform-specific targeting and function, suggesting that V5 domains might represent novel targets for pharmaceuticals designed to regulate PKC isoform-specific signaling in cells (Steinberg, 2008).

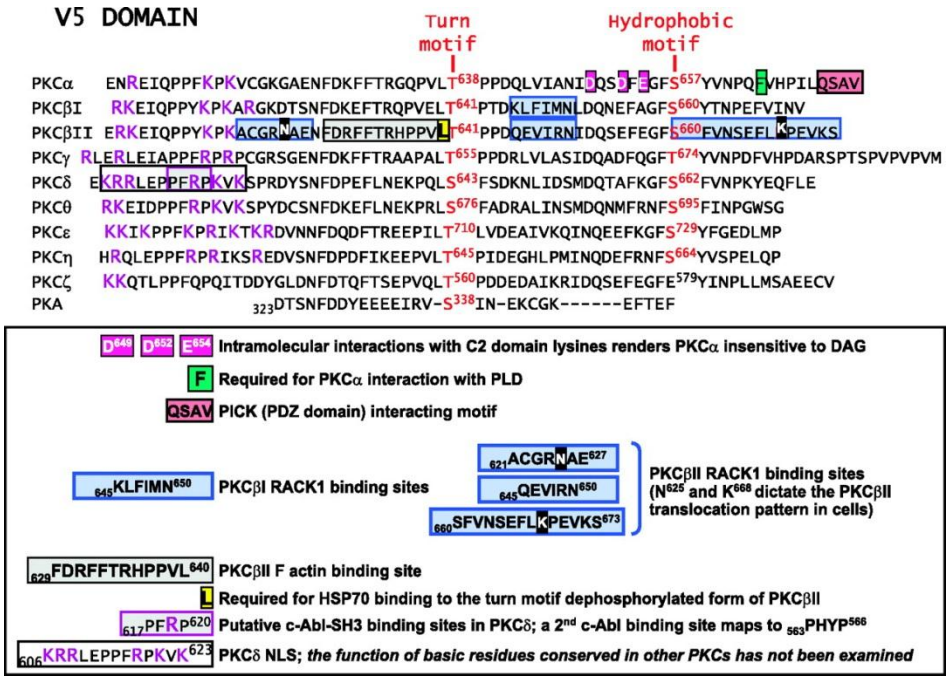

Figure 4**.** Alignment of the V5 domain in PKC isoforms (Adopted from Steinberg, 2008).

The binding of PKC to other kinases provides a mechanism for cross-regulating the phosphorylation state and activity of different signaling pathways in somatic cells (Jaken and Parker, 2000; Koeneman and Capco, 2004). For example, in addition to PKC, glycogen synthase kinase 3β (GSK3β) is a regulator of microtubule stability, and GSK3β needs to be inactivated to maintain the mitotic spindle. Apart from the role of GSK3β in the Wnt signaling pathway, several studies have also pointed towards a role for GSK3β in the regulation of microtubule dynamics. In neuronal cells, GSK3β is able to phosphorylate a number of microtubule-associated proteins, such as MAP2C, MAP1B and Tau (Lovestone et al. 1996; Goold et al. 1999; Sanchez et al. 2000) as seen in the

representative diagram in figure 5. This figure is an outline of the various substrates of GSK3α/β. Phosphorylation of the MAP proteins by GSK3β decreases their ability to stabilize microtubules (Lovestone et al. 1996; Wagner et al. 1996; Utton et al. 1997). Earlier studies have shown that inactivation of GSK3β in mitotic cells permits microtubules to be present (Wakefield et al. 2003). In other cells, when GSK3β is activated, microtubules are destabilized (Goold et al. 1999; Jope and Johnson, 2004). Moreover, GSK3β is a known substrate for PKCζ (Etienne-Manneville and Hall, 2003; Krishnamurthy et al. 2007). An earlier study indicated that PKCζ acts through GSK3β in mouse oocytes to mediate spindle stability (Baluch and Capco, 2008).

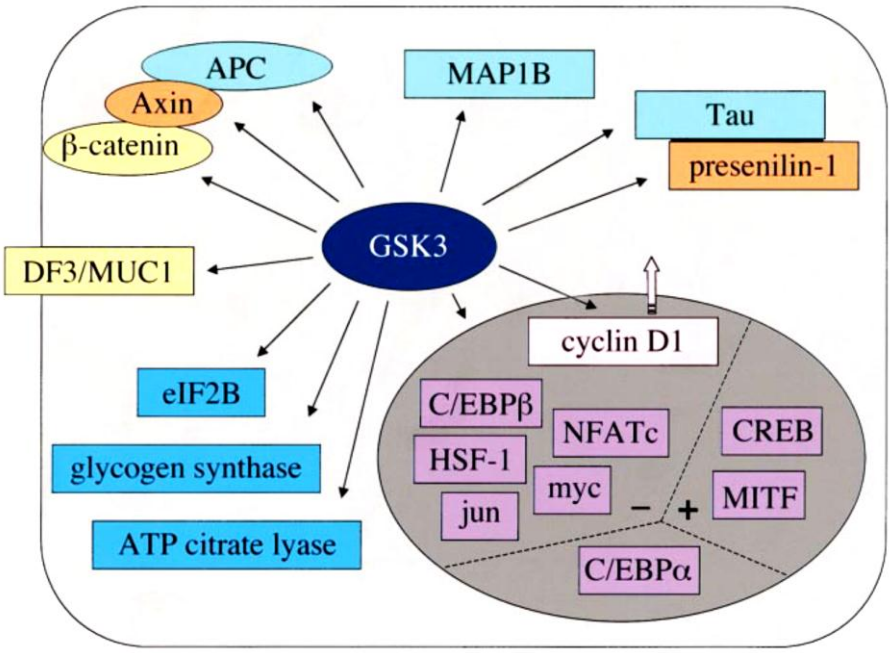

Figure 5: Substrates of GSK3. Putative substrates are color-coded according to their proposed function in the cell ; transcription factors (mauve), enzymes that regulate metabolism (blue), proteins bound to microtubules (turquoise), scaffold proteins (orange), or components of the cell division cycle machinery (pink) or

involved in cell adhesion (yellow). Transcription factors are subdivided into those that are inhibited (+), activated (-) or unaffected by the phosphorylation by GSK3. (Adopted from Frame and Cohen, 2001).

In Chapter 2, studies were conducted to test the hypothesis that when compared to the other PKC isoforms, phospho-PKCζ (pPKCζ) is the likely isoform to interact with GSK3β to regulate mitotic spindle stability. The metaphase stage of mouse fibroblast cells with a centrosomal spindle was used for these studies. In these studies, co-localization and molecular proximity between pPKCζ and inactive GSK3β in the centrosomal region was first tested. Next inhibitors of pPKCζ were used in further studies in order to study if pPKCζ acts with GSK3β to disrupt the proteins involved in maintaining the mitotic spindle. Evidence is provided to show that pPKCζ may act through GSK3β to permit the spindle apparatus to exist at the metaphase stage in a centrosomal spindle.

Apart from PKC and GSK3β, in mammalian mitosis, the role of mitogen activated protein kinase (MAPK) pathway in cell cycle regulation has been extensively examined. For example studies indicate that activation of the MAPK pathway is required for normal progression into mitosis (Guadagno and Ferrell, 1998; Wright et al. 1999; Hayne et al. 2000). Besides mitosis, the MAPK pathway is involved in a multitude of functions including cell cycle regulation, cell differentiation, and cell death in eukaryotes ranging from yeast to humans (Nigg et al. 2001; Orton et al. 2005; Rozengurt, 2007; Marks et al. 2009). As part of this pathway, many somatic cell studies have shown that Raf kinase activates MEK1/2 (MEK) by phosphorylation of two serine residues. MEKs generally

recognize only MAPKs as substrates. It has been reported that MEK has a 'TEY' motif within its activation loop (Yung et al. 1997, Orton et al. 2005).

It has been reported that activated MEK and ERK localize to the centrosomes of the mitotic spindle from prophase to anaphase, and to the mid-body during cytokinesis (Shapiro et al. 1998; Willard and Crouch, 2001; Collelo et al. 2012). ERK, the known downstream target of MEK has been shown to be associated with the centrosome and kinetochore components of the mitotic spindle apparatus, and has multiple functions during mitosis including, promoting mitotic entry as well as targeting proteins that mediate mitotic progression in response to kinetochore attachment (Schmidt-Alliana et al. 1998; Shapiro et al. 1998; Saffery et al. 2000). Activated ERK co-localizes with the kinetochore motor protein CENP-E, raising the possibility that CENP-E is a downstream effector for ERK during mitosis (Zecevic et al. 1998; Willard and Crouch, 2001; Chambard et al. 2006). Studies have shown that blocking MEK activity in cycling somatic cells does not significantly affect mitotic entry, but it does slow progression through mitosis, probably by slowing the CENP-E-dependent chromosome movements coordinated by the mitotic spindle (Roberts et al. 2002). Other studies have shown that active MEK along with active cyclinB-Cdc2 is necessary for the cells to progress into M-phase (Harding et al. 2003; Walsh et al. 2003).

Signaling networks are important for cell proliferation, and communication between pathways can take place at many locations from the plasma membrane to the nucleus. Signaling network is increasingly important for our understanding of cell proliferation. Cross-talk involves components that are

in common pathways, as well as positive and negative feedback signals. The MAPK pathways are tightly regulated by and cross-communicate with other signaling pathways. An overview of the other cellular pathways that communicate with the MAPK pathway is shown in figure 6. Figure 6 indicates cross-talk between the MAPK pathway, the Glycogen synthase kinase 3β (GSK3β) pathway and the protein kinase C (PKC) pathway (Nigg, 2001; Zhang and Liu, 2002; Kholodenko, 2006; Rozengurt, 2007). GSK3β and PKC have been found to be associated with the mitotic spindle (Lehrich and Forrest, 1994; Etienne-Manneville and Hall, 2003; Wakefield et al. 2003; Jope and Johnson, 2004; Liu et al., 2006; Kalive et al. 2011). Earlier studies have shown that GSK3β is associated with the centrosome and is known to phosphorylate microtubule associated proteins (MAPs) such as MAP1B which in turn causes chromosomal segregation by the microtubules. In these studies the MAPK pathway was shown to be upstream of GSK3β (Goold et al. 1999; Frame and Cohen, 2001; Goold et al. 2005; Scales et al. 2009).

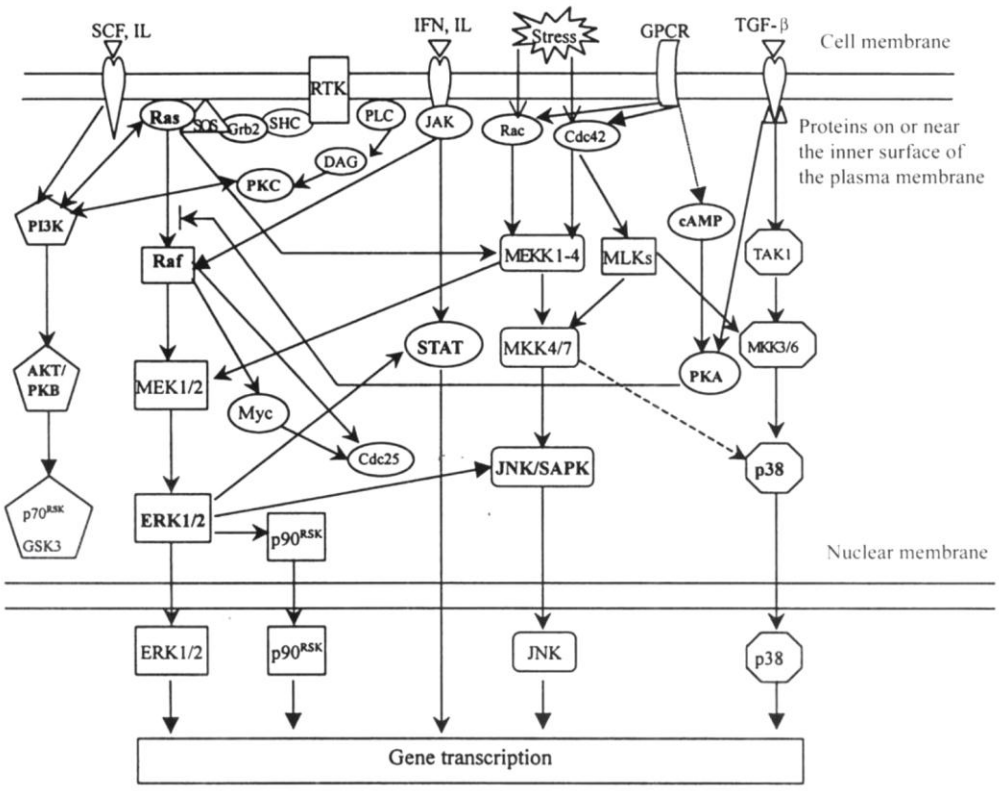

Figure 6: An overview of MAPK pathways involved in a signaling network in mammalian cells (Adopted from Zhang and Liu, 2002).

PKCs also have been reported previously as upstream activators of the MEK/ERK pathway (Brändlin et al. 2002; Puente et al. 2006; Chang et al. 2008; Marks et al. 2009). In an earlier study the PKCζ isoform has been implicated to be an upstream activator of MEK (Berra et al. 1995; Short et al. 2006). In addition, the PKCζ isoform has been shown to be associated with the centrosome region of the mitotic spindle, or with the spindle microtubules (Lehrich and Forrest, 1994; Liu et al. 2006), and its activation is known to play an important role in stable kinetochore-microtubule attachment and subsequent chromosomal

separation (Liu et al. 2006). PKC isoforms can directly regulate Raf-1 which is an upstream activator of the MEK/ERK pathway, specifically PKCα and PKCη are known activators of Raf-1 (Schonwasser et al. 1998; Corbit et al. 2003). A previous study showed that inhibition of active PKCζ by a myristoylated peptide inhibitor causes inhibition of p(ser9)GSK3β at the centrosomes and disruption of the mitotic spindle. This study also suggests that p(ser9)GSK3β could be a substrate of active PKCζ (Kalive et al. 2011). However, no single study has examined all four of the kinases at the same time in the same cell type.

In Chapter 3, studies were conducted to determine the involvement of MEK, ERK, GSK3β and PKCζ in regulation of the mitotic spindle. In these studies, MEK and ERK activity were separately inhibited in the same cell type and it was determined whether this inhibition affects the location and activity of PKCζ and GSK3β. If MEK/ERK, PKCζ, and GSK3β interact then we predicted that they would co-localize at the spindle during mitosis. Moreover, if MEK and ERK have sole control over the mitotic spindle then inactivation of either MEK or ERK may obliterate the spindle followed by a slower progression through mitosis. In contrast, if multiple signaling pathways are involved then a modification or reduction in the spindle might be observed followed by only a reduction in the progression through mitosis.

Chapter 2

INVOLVEMENT OF PKCZETA AND GSK3BETA IN THE STABILITY OF THE METAPHASE SPINDLE

Madhavi Kalive, D. Page Baluch, David G. Capco

Introduction

Protein Kinase C (PKC) has been implicated in a wide range of G protein-coupled receptor mediated responses, growth factor-dependent cellular responses, and is comprised of a family of isoforms that subserve unique or sometimes opposing functions in cells, (Steinberg, 2008). PKC is a family of 11 isozymes that are classified into three subfamilies depending on their structural similarity and cofactor requirements. The regulatory domains are different among the various isoforms, which contributes to a variety of roles played by the PKC isoforms, (Roffey et al. 2009; Rosse et al. 2010). The conventional PKCs namely, PKC α, βI, βII, and γ are diacylglycerol (DAG), phospholipid, and calcium dependent. The novel PKCs are DAG and phospholipid dependent but are calcium independent and include PKC ε, η, μ, θ, and δ. The atypical PKCs are DAG and calcium independent and include PKCζ and human PKCι / mouse PKCλ, (Liu et al. 2006). Two new isoforms of PKCζ, namely PKMζ which has a new PKCζ catalytic domain has been described in the brain, (Hernandez et al. 2003) and PKCζII is involved in cell polarity, (Parkinson et al. 2004). Each PKC isoform is involved in regulating specific cellular functions based on subcellular location and binding properties. The interaction of PKC with other proteins in

cytoskeletal compartments has been shown which supports a role for PKC in cytoskeletal reorganization, (Jaken and Parker, 2000).

The mitotic spindle apparatus of a somatic cell is 'centrosomal' (Debec et al. 2010); (Walczak et al. 2010), wherein there are centrosomal structures at each spindle pole. This is contrasted, for example, with mammalian oocytes where the meiotic spindle apparatus is 'acentrosomal', and lacks the centrosomal structures. The mitotic spindle is a dynamic molecular structure, composed of tubulin, motors, and other associated proteins, (Karsenti and Vernos, 2001; Debec et al. 2010); Walczak et al. 2010) and studies have shown microtubule associated proteins as substrates of PKC, (Robinson et al. 1991; Correas et al. 1992). Moreover, phorbol esters which are activators of PKC have been shown to cause microtubule reorganization, (Kiley and Parker, 1997). Some of the PKC isoforms have been shown to be associated with the microtubules or the centrosome of the spindle apparatus although their role in spindle stability has not been elucidated. These include PKC βI, βII, ε, θ, δ and ζ, (Lehrich et al. 1994; Kiley and Parker, 1995; Volkov et al. 1998; Passalacqua et al. 1999; Takahashi et al. 2000; Chen et al. 2004; Eng et al. 2006; Liu et al. 2006).

The binding of PKC to other kinases provides a mechanism for cross-regulating the phosphorylation state and activity of different signaling pathways in somatic cells, (Jaken and Parker, 2000; Koeneman and Capco, 2004). For example, in addition to PKC, Glycogen Synthase Kinase 3β (GSK3β) is a regulator of microtubule stability and GSK3β needs to be inactivated to maintain

the mitotic spindle. Earlier studies have shown that inactivation of GSK3β in mitotic cells permits microtubules to be present, (Wakefield et al. 2002). In other cells, when GSK3β is activated, microtubules are destabilized, (Goold et al. 1999; Jope and Johnson, 2004). Moreover, GSK3β is a known substrate for PKCζ, (Etienne-Manneville and Hall, 2003; Krishnamurthy et al. 2007).

Based on these previous studies, we hypothesize that when compared to the other PKC isoforms, phospho-PKCζ (pPKCζ) is the likely isoform to interact with GSK3β to regulate mitotic spindle stability in the metaphase stage of mouse fibroblast cells with a centrosomal spindle. If this hypothesis is correct, two predictions should follow: 1) there should be significant co-localization and molecular proximity between pPKCζ and inactive GSK3β in the centrosomal region and, 2) inhibitors of pPKCζ act with GSK3β to disrupt the proteins involved in maintaining the mitotic spindle. The results reported in this study support these predictions. Evidence is provided to show that pPKCζ may act through GSK3β to permit the spindle apparatus to exist at the metaphase stage in a centrosomal spindle.

Materials and Methods

Cell culture and media

The cells used for all the experiments were NIH 3T3 mouse fibroblasts, ATCC number CRL-2795. The cells were maintained at 10% CO2 concentration in a 37^0C moisture incubator. DMEM media was used to maintain the cells (10% fetal calf serum (FCS), 1% Penicillin-streptomycin, 2% L-glutamine). The cells

were grown to 80% confluency before being used. All chemicals used in experiments were obtained from sigma unless otherwise indicated.

Inhibitor treatment

A dose response analysis was performed in order to determine the amount of inhibitor to be added to the cells and the time of exposure. Metaphase synchronised 3T3 cells were subjected to logarithmically increasing concentrations of the inhibitor at a one hour time point and then subjected to immunocytochemical analysis using the pPKCζ specific antibody, then viewed by confocal microscopy. The optimal concentration of the inhibitor was determined. The lowest possible concentration that completely suppressed pPKCζ was used. The inhibitor, myristoylated PKCζ pseudosubstrate (EMD Corp., La Jolla, CA), was diluted to the working concentration of 50μM (as determined by the dose response analysis) in DMEM media. The 3T3 cells were treated with the inhibitor for 30min and for 1hr. and processed for further immunocytochemical analyses or for immuno-pull down assays followed by western blotting. For the experiment involving the addition of both PKCζ inhibitor and GSK3β inhibitor, the PKCζ inhibitor was added at 50μM concentration for 1hr. followed by 2.5μM GSK3β peptide inhibitor (Calbiochem Corp., La Jolla, CA) for 1hr in fresh media. All experiments were repeated three times independently.

GSK3β kinase permeabilization assay

The cells were permeabilized by washing briefly in modified ICB (100mM KCl, 5mM MgCl2, 5mM BAPTA, 20mM HEPES [pH 6.8] made 1% with Tween-20 and 1μg/mL each of pepstatin, aprotinin, chymostatin, leupeptin, and trypsin- chymotrypsin (Sigma Chemical Co., St. Louis, MO). After permeabilization, the cells were washed briefly with modified ICB without Tween-20 to remove the detergent. The cells were incubated with 40ng/mL GSK3β kinase and 1mM ATP (Cell Signaling Technology Inc., Danvers, MA) made in modified ICB (with added protease inhibitors) without Tween-20 for the indicated time points. Parallel samples were incubated with the combination of GSK3β kinase and 1mM ATP in modified ICB without Tween-20 along with 2.5μM GSK3β peptide inhibitor (Calbiochem Corp., La Jolla, CA). Samples were then fixed with 2% paraformaldehyde in ICB, prepared for immunocytochemistry and confocal imaging. To view the spindle, antibody to α-tubulin (Sigma Chemical Co., St. Louis, MO) was used. To view the chromosomes of the cells, DRAQ 2.4μg/mL in ICB (Axxora, LLC, San Diego, CA) was used. The experiments were repeated three times independently and every time, fifty cells at the metaphase stage were scored in each assay.

Collection of cells at mitotic metaphase

Cells at 80% confluency were treated with nocodazole at 10μM made in DMEM media for 14-16hrs at 37^0C, (Jackman and O'Conner, 1998). After removal of the nocodazole media, cells were rinsed once briefly with DMEM

media without nocodazole, then allowed to recover in fresh DMEM media for 30mins. Cells were then subject to a 'mitotic shake', each T-flask (T75 flask) for about 4min. The cells as a pellet were then recovered by spinning at 3000rpm for 10min. RIPA buffer with protease inhibitors was used to make the cell lysate as described below.

Immunopurification (Immuno-pull down assays)

The Catch and Release Reversible Immunoprecipitation System v2.0 (Millipore, Inc., Lake Placid, NY) was used according to the manufacturer's instructions. In the procedure, the number of cells used per experiment was kept constant. For every Immunoprecipitation column, 1 T-flask was used with cells grown to 80% confluency. After the appropriate treatment, the cell lysate from each T-flask was made in 500μL of cold RIPA lysate buffer (Pierce Biotechnology, Rockford, IL) with 1μg/mL of aprotinin, pepstatin, chymostatin, leupeptin and trypsin-chymotrypsin (Sigma Chemical Co., St. Louis, MO). The lysate was added to the immunoprecipitation column along with 2μg of either pPKCζ antibody or p(ser9)GSK3β antibody and 10μL of the affinity ligand. The column was gently rocked overnight at 4^{o}C. After 3 washes with the buffer provided, 70μL of the non-denaturing elution buffer was used to elute the immunoglobulin complex. This was analysed by SDS- PAGE and western blotting using the appropriate primary and secondary antibodies.

Western analysis

A Bradford assay was performed in order to determine the concentration of protein that was loaded onto the SDS gel. The samples used for the immunopurification Western gels were loaded at a concentration of 750µg/ml in each lane. Laemmli 2X sample buffer was added to cell lysate samples, inhibitor treated cell lysate samples or immunopurified cell lysate samples, (Laemmli, 1970). The samples were kept in a boiling water bath for 10min to denature the proteins. The samples were then loaded onto a pre-cast 10% Tris-HCl precise protein gel (Pierce Biotechnology, Rockford, IL), then transferred to a PVDF membrane, (Towbin et al. 1979). The Kaleidoscope protein dye was used as the marker to confirm molecular weight. The blot was blocked in BLOTTO (5% non-fat dried milk in PBS-T [PBS with 0.1%Tween-20] was used as the blocking agent for the blot for 1 hour, the blot was rinsed and treated with the appropriate primary antibodies at a 1:500 concentration overnight at 4^{O}C. The blot was then washed 3 times with PBS-T the following day. The appropriate rat HRP or rabbit HRP (Pierce Biotechnology, Rockford, IL) were applied to the blot as secondary antibody in BLOTTO for 2hrs at room temperature. After washing the blot with PBS-T 3 times, chemiluminescence was used to detect the protein bands on the blot. The ECL plus kit (formerly Amersham Biosciences, Arlington, IL) and the Hyperfilm ECL chemilumiscent film (GE Healthcare) were used for the detection.

Immunocytochemistry

The living (i.e. intact) 3T3 mouse fibroblast cells were fixed intact for 30min in 2% formaldehyde in ICB (ICB: 100mM KCl, 5mM $MgCl_2$, 3mM EGTA and 20mM HEPES (pH 6.8), in H_2O) and permeabilized for 1hr in ICB with 2% paraformaldehyde and 1% Tween-20. The samples were then washed 3 times for 15min each wash with ICB-BSA buffer (1% BSA in ICB). Primary antibodies were then added to the cells in the antibody dilution buffer (1% non-fat milk, 0.5% Tween-20 in ICB) at a 1:500 dilution for each antibody overnight at 4^0C with gentle rocking. The following day, the cells were washed with the ICB-BSA buffer 3 times 15min each wash with gentle rocking. The appropriate secondary antibodies were added to the cells overnight at 4^0C with gentle rocking. The secondary antibodies were made in the antibody dilution buffer at a 1:1000 antibody concentration. The following day, cells were washed with the ICB-BSA buffer 3 times 15min each wash, then placed in DRAQ5 (2.4μg/mL in ICB [AXXORA, LLC San Diego, CA]) for a 15min incubation. This was done to visualize the chromosomal material microscopically. The primary antibodies used were: anti-pPKC βII, anti-pPKC δ, anti-pPKC ζ, anti-p(ser9) GSK3β (Santa Cruz Biotechnology, Santa Cruz, CA). pPKC γ, pPKC α, pPKC μ, pPKC θ (Cell Signaling Technology, Beverly, MA). The secondary antibodies used were Alexa-568 and 488 – conjugated IgGs (Molecular Probes, Inc, Eugene, OR).

In order to perform the detergent extraction procedure, 3T3 mouse fibroblasts were treated with a detergent extraction buffer (Intracellular buffer made 1% Tween-20 and AEBSF at 200μg/ml as a protease inhibitor) for 5min.

This permitted the cytoskeletal components of the cells to be retained and the soluble components to be released into the media which was removed, (Capco et al. 1987). Cells were then fixed and permeabilized for immunocytochemistry as described above.

Confocal microscopy

The cells were mounted on coverslips sealed with nailpolish after the immunocytochemistry procedure. The cells were viewed on the Leica SP2 microscope in the W. M. Keck Bioimaging Laboratory at Arizona State University. For each experiment, fifty cells were observed. Multiple lasers allowed for simultaneous imaging of the Alexa 488 and Alexa 568 (Argon 488nm; Krypton 568nm) fluorophore labeled samples. Using a 100X oil objective, images were scanned at 0.5μM slices in the z-axis at the spindle region. The image files were analyzed and intensity ratios calculated using the Leica NTS software. (Leica Microsystems, Bannockburn IL). In order to calculate the pixel intensity scan ratios, a square from the Leica software was used as the "reference frame" in each cell from which the pixel intensity numbers were derived via the Leica software. In order to calculate the ratio of the pixel intensities at the centrosome vs the pixel intensity at the cytoplasm, the dimensions of the "reference frame" were kept constant and also the location on the cytoplasm was kept constant across cells. For co-localization experiments, only the yellow pixels were used to calculate the pixel intensity ratios.

Fluorescence resonance energy transfer measurements (FRET)

Cells labeled with the appropriate primary and secondary antibodies were used. After immunocytochemistry the cells were viewed on the Leica SP2 confocal microscope housed in the W.M. Keck Bioimaging Facility at Arizona State University. Multiple lasers allowed for sequential imaging of Alexa 488 (Argon [488nm]) and Alexa 568 (Krypton [568nm]) fluorophore labeled samples. FRET analysis was carried out using the FRET acceptor bleaching software in the Leica SP2 confocal imaging system. The energy efficiency of the donor by acceptor photobleaching was calculated by the software, (Zimmerman et al. 2002). The FRET efficiency was calculated using the formula:

FRETeff = Dpost – Dpre / Dpost for all Dpost > Dpre

Where: D represents the emitted donor fluorescence before and after bleaching.

The acceptor fluorophore (Alexa 568) was photobleached to 100% so that it was indistinguishable from background fluorescence. FRET trace images were also generated for each pair scanned. These highlight the regions of FRET interaction based on a colorimetric scale.

Results

Localization of pPKC isoforms at the mitotic spindle

The mitotic spindle of mouse 3T3 fibroblasts was challenged with antibodies to different phospho-PKC isoforms (pPKC), that is, antibodies that bind to the active forms of the kinase (Fig. 7 a-o). Antibodies to pPKCζ and pPKCδ (Figs. 7m and 7g respectively) were highly enriched at either side of the metaphase plate where the centrosomal spindle pole would be located. To confirm that these were the centrosome, dual labeling with pericentrin (green) and pPKCζ (red) was conducted. The inset in figure 7m shows the yellow centrosome as a co-localization of the individually labeled pericentrin and pPKCζ. The pPKCα, βII, μ, and θ isoforms also were enriched at the centrosome but to a lower extent. In contrast, pPKCγ (Fig. 7e) appeared to be enriched along the spindle microtubules and to a lesser extent at the centrosome. The association of pPKC isoforms with the spindle or centrosome in intact cells suggested that the isoforms may be physically connected to the centrosome. To test this, living cells were detergent extracted, a process where soluble components are removed and components associated with the detergent-resistant cytoskeleton are retained. Subsequently when cells were cytologically fixed and then challenged with antibodies to the pPKC isoforms, the ζ and δ isoforms remained highly enriched at the centrosome (Fig. 7n, h respectively) while the pPKCθ isoform was absent from the centrosome (Fig. 7l). The α, βII, μ, and θ isoforms of pPKC also remained at the spindle pole though at a lesser intensity than the ζ and δ isoforms.

Detergent extraction also resulted in the reduction of pPKCγ binding to the spindle microtubules.

The extent of enrichment at the centrosomal poles was standardized by comparing the pixel intensity at the centrosomal pole to the pixel intensity in the remainder of the cytoplasm (Fig. 7o). This ratio permitted the quantitation of relative amounts of pPKC isoforms on the mitotic spindle as measured by the signal intensity ratio of the pPKC isoform antibody labeling. The ratio was obtained by conducting a pixel intensity scan through the spindle and separately through the cytoplasmic area in multiple cells from different experiments. Each cell was sampled at three sites at the centrosomal pole and three sites elsewhere in the cytoplasm in three independent experiments, with the exception of the pPKCθ isoform, which had no enrichment at the centrosomes after detergent extraction. The intensity ratio for the enrichment of both pPKCζ and pPKCδ at the centrosome was significantly greater than the intensity ratio for the enrichment of the other pPKC isoforms.

Unlike the other pPKC isoforms, pPKCζ also could be seen in an array of spots at the metaphase plate in the region of the chromosomes (Fig. 7m, arrow). This localization of pPKCζ at the region where chromosomes are found was detected by utilizing the technique of 'frame averaging' while scanning with the confocal microscope in order to reduce background noise and enhance the clarity of pPKCζ signal enrichment. In figure 7 the mouse fibroblasts also were assessed for the enrichment of all the phospho-isoforms using the frame-averaging

technique. As noted above only pPKCζ showed enrichment in the region of the chromosomes after frame averaging (Fig. 7m intact and detergent extracted).

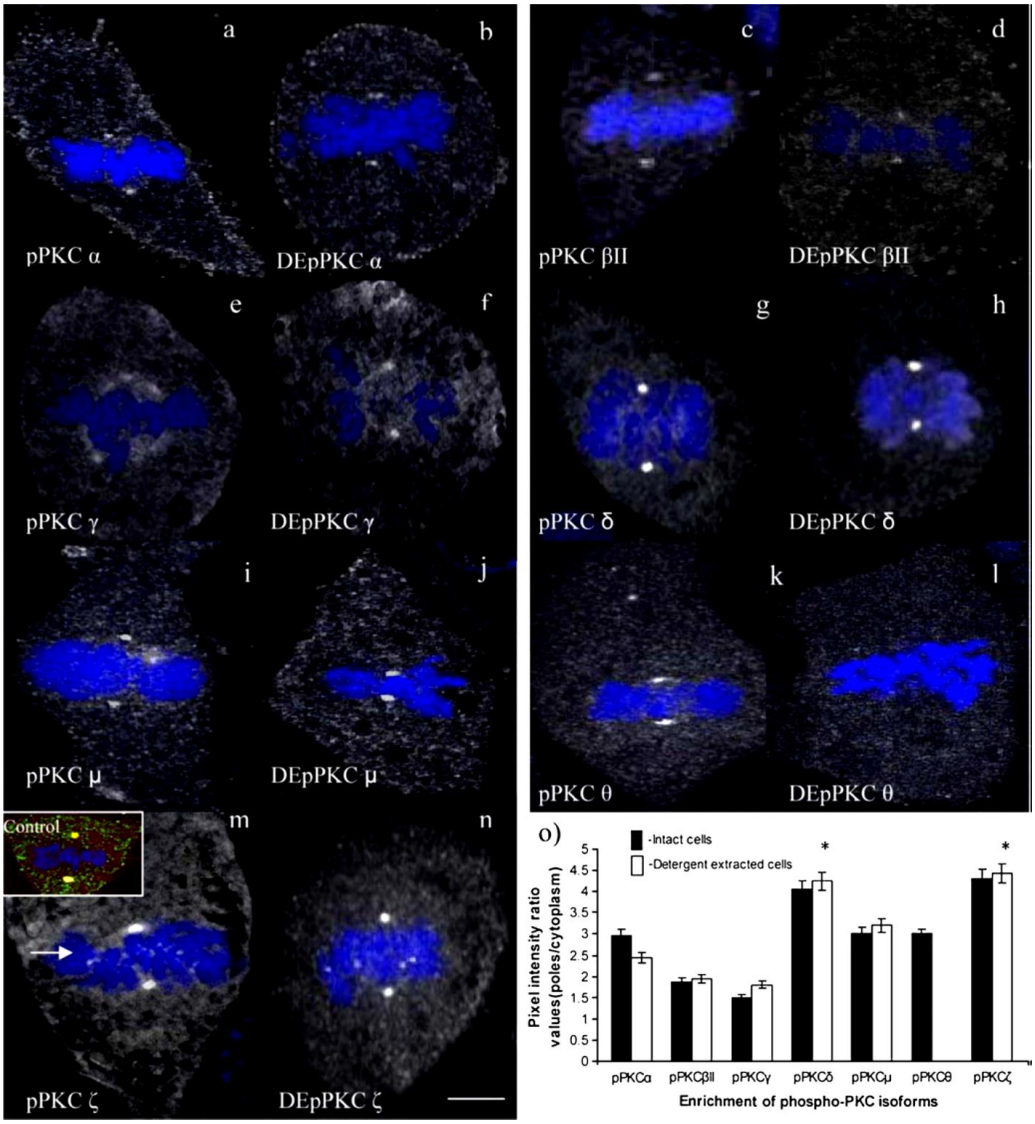

Figure 7. Enrichment of phospho(p)-PKC isoforms in 3T3 metaphase cells—intact and detergent-extracted (DE). (a, c, e, g, i, k, m) In intact cells and (b, d, f, h, j, l, n) detergent-extracted (DE) cells, the localization of pPKC isoforms can be seen in gray tones and the chromosomes are stained blue with DRAQ5. All confocal images shown are frame averaged single optical sections. (m) Phospho-PKCζ has the highest localization intensity at the centrosome in intact and (n) DE

cells and also in the region where the chromosomes are found (in intact cells indicated by an arrow, m). Inset (m) shows control cell co-labeled with pericentrin and pPKCζ at the centrosome. The other pPKC isoforms localize at the centrosome, in intact cells and DE cells at mitotic metaphase. (l) Phospho-PKCθ does not localize at the poles after detergent extraction. (e, f) Phospho-PKCγ localizes along the spindle structure. (o) A graphical representation of the pixel intensity ratios is shown. Pixel intensity ratios are expressed as the mean±SEM (n03). A total of 50 cells were analyzed for each PKC isoform. Means were compared using the Student's unpaired t test. The value for pPKCζ and pPKCδ is significantly higher than the other pPKC isoforms ($P<0.002$). Scale bar is 10 μm.

Co-localization of pPKCζ and p(ser9)GSK3β and FRET analysis

Earlier studies conducted in yeast, Drosophila, C. elegans and various somatic cell lines have found that the interaction of the atypical PKCζ and GSK3β has a key role in specific signaling pathways, Etienne-Manneville and Hall (2003); Krishnamurthy et al. (2007); Kim et al. (2007). The enrichment of p(ser9)GSK3β and pPKC isoforms was demonstrated at the centrosome by labeling the cells with a p(ser9)GSK3β specific antibody and pPKC isoform specific antibodies (Fig. 8, panels a, b, c and d). The enrichment of pPKC isoforms was shown in the red channels and the enrichment of p(ser9)GSK3β was shown in the green channel, thus co-localization between the two would appear yellow in the merged image. In figure 8, panel a, the cells at metaphase were double labeled with antibodies to pPKCζ and p(ser9)GSK3β and in order to better visualize the signal of pPKCζ and p(ser9)GSK3β at the chromosomal region, the blue channel visualizing the chromosomes was turned off. The arrows shown in each channel of panel 8a indicate the region of the chromosomes. Yellow spots can be seen both at the centrosomal region and the chromosomal region. The inset in figure 8 panel 'a' shows a control cell co-labeled with antibodies to

pericentrin (green) and pPKCζ (red) to indicate the co-localization at the centrosome as yellow. When the other pPKC isoforms were used, such as, pPKC α, βII, γ, (Fig. 8 panels b, c, and d respectively) this area showed few yellow pixels indicating little co-localization. To quantify this amount of co-localization at the centrosome, pixel intensity scan ratio of the centrosome vs the cytoplasm in the merged channel quantifying only the yellow pixels was calculated and the results shown as a histograph in figure 8e. The 'yellow pixel intensity scan ratio' allowed for the comparison of the signal intensities of each pPKC isoform antibody co-labeled with p(ser9)GSK3β antibody. Each cell was sampled at three sites on the centrosomal pole and three sites elsewhere in the cytoplasm in three independent experiments. The pixel intensity ratio of yellow pixels at the poles is highest for pPKCζ, while the other isoforms show less yellow pixel intensity at the centrosome. Cells that were co-labeled with pPKCζ and p(ser9)GSK3β were also examined for co-localization at the chromosomal region by the frame averaging technique. The co-localization can be seen at the chromosomal region as yellow spots in figure 8a (merged channel). The other pPKC isoforms did not exhibit a co-localization with p(ser9)GSK3β.

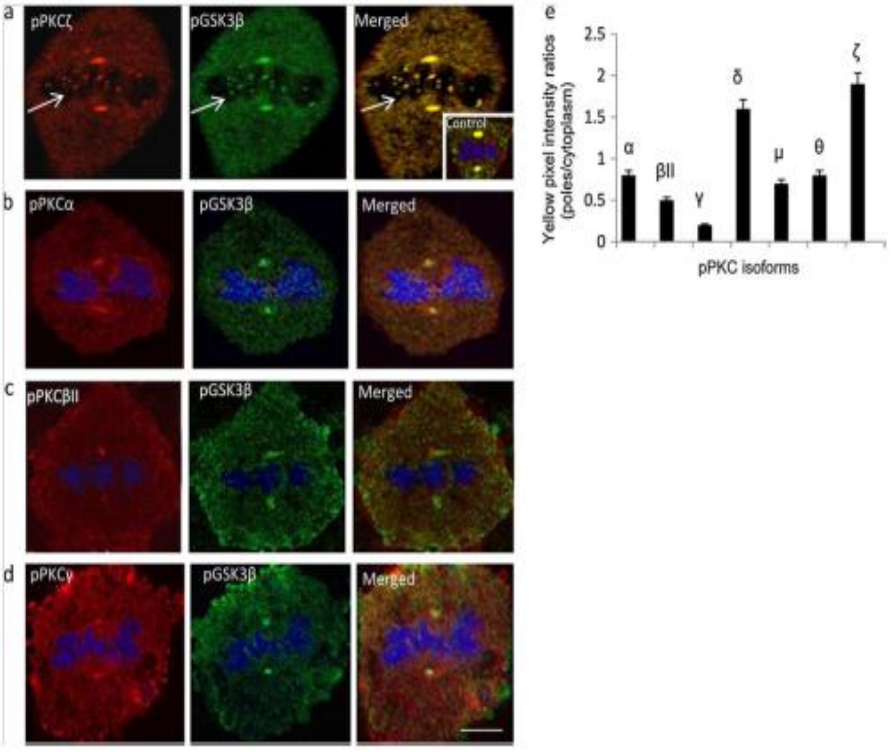

Figure 8. Co-localization of the different phospho isoforms of PKC with p(ser9)GSK3β. (a) The PKC isoform, pPKCζ (red) was tested for co-localization with p(ser9)GSK3β (green) at the mitotic metaphase stage by immunocytochemistry and con-focal microscopy. The blue channel to show chromosomes was turned off to permit clear viewing of the signal at the region of the chromosomes, which can be seen as dark areas in the shape of chromosomes. The merged image indicates co-localization seen as areas showing yellow pixels. The arrows in (a) indicate co-localization of pPKCζ and p(ser9)GSK3β at the region of the chromosomes. (b, c, d) Other pPKC isoforms (red) such as pPKCα (b), pPKC βII (c), pPKC γ (d) were also tested for co-localization with p(ser9)GSK3β (green). The cells are triple-labeled with p(ser9)GSK3β (green), pPKC isoform (red), and DRAQ5 (blue) to show the chromosomes. The areas of co-localization are yellow as seen in corresponding merged images. The inset in (a) is a merged image of a control cell to show the co-localization of pPKCζ and pericentrin at the centrosome. Co-localization is indicated by yellow pixels at the centrosome. (f) The histogram shown is a pixel intensity graph with the yellow pixel intensity ratio (average yellow pixel scan of centrosome/average pixel scan of cytoplasm) of the co-localization. Some of the pPKC isoforms shown in the histogram are not shown in the confocal images such as pPKCδ, pPKCμ, and pPKCθ. Yellow pixel intensity ratios are expressed as the mean±SEM (n03). Means were compared using the Student's unpaired t test. The values for pPKCζ and pPKCδ colocalization are significantly higher than the

other pPKC isoforms ($P < 0.002$). The confocal images shown are single optical sections. Scale bar is 10 μm.

To confirm that pPKCζ and p(ser9)GSK3β were in close association, fluorescent resonance efficiency transfer (FRET) was performed. Close molecular proximity would permit the possibility that the proteins could interact for example enzymatically. Energy transfer can occur only if two protein targets are within 10-100 Å. Even a small FRET value indicates the evidence of molecular proximity whereas co-localization data does not confirm such a close association. FRET was measured both at the centrosome and the chromosomal region for all the PKC isoforms with p(ser9)GSK3β. FRET measures increased fluorescence intensity in a fluorescent donor when the fluorescent acceptor is bleached. FRET results do indicate that there is close molecular proximity between pPKCζ and p(ser9)GSK3β with an average FRET value of 33.51% at the poles and an average of 47.2% at the chromosomal region (Fig. 9a). FRET also was detected between pPKCδ and p(ser9)GSK3β co-localization with an average value of 4.56% at the poles and an average value of 5.27% at the chromosomal region, while the FRET values for the other pPKC isoforms are not detectable. The boxes in figure 9 b, c, d, e, indicate the regions tested for FRET. These results provide evidence that in a centrosomal spindle as found in the mouse fibroblast cell, pPKCζ and p(ser9)GSK3β are in close proximity. In order to confirm that these spots above and below the chromosomes represent the centrosome, separate experiments were conducted to test FRET between pPKCζ and γ-tubulin (enriched in the centrosome) and between pPKCζ and pericentrin (a

centrosome-specific marker). Both experiments gave detectable FRET values at the centrosome supporting the notion that these are the centrosomes (Fig. 9a).

a.

FRET Pair	FRET value at spindle poles	FRET value at chromosomal region
pPKC ζ – pGSK3 β	33.51%	47.2%
pPKC δ – pGSK3 β	4.56%	5.27%
pPKC ζ – Pericentrin	5%	0%
pPKC ζ – γ-tubulin	8%	0%

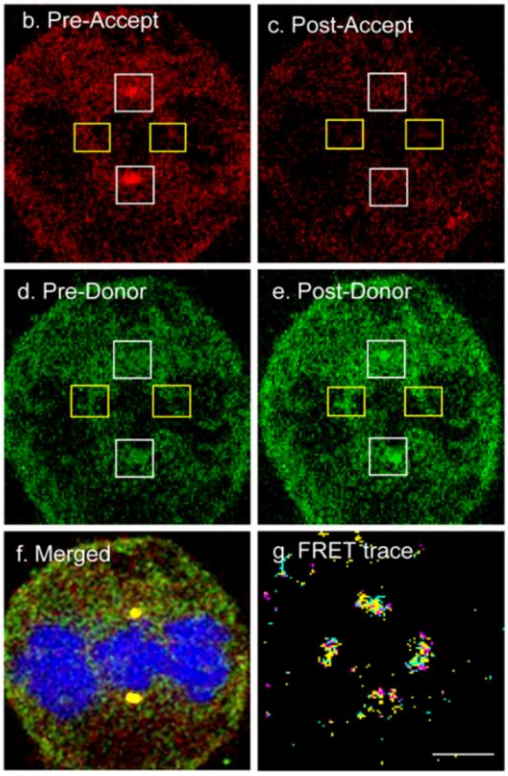

Figure 9. FRET values measured between pPKCζ or pPKCδ and p(ser9)GSK3β at metaphase stage of 3T3 cells. (a) The table indicates the average FRET values at the spindle pole regions and at the chromosomal regions for pPKCζ or pPKCδ double-labeled with p(ser9)GSK3β at mitotic metaphase. (b, c) A representative pre-and post-bleaching image of the FRET process for pPKCζ and (d,e) for p(ser9)GSK3 β are shown. The white boxes in the images (b, c, d, e) indicate the regions tested at the centrosome; the yellow boxes (b, c, d, e) indicate the regions tested at the chromosomes. (f) A pre-bleached merged image of the pPKCζ co-labeled with p(ser9)GSK3β is shown in comparison to (g) the FRET trace image. Scale bar is 10 μm.

Immuno-pull down studies to show p(ser9)GSK3β – pPKCζ isoform interactions

An immuno pull-down assay was performed to further confirm that pPKCζ is associated with p(ser9)GSK3β in these cells. The cell lysates used were prepared from 3T3 cells synchronized to metaphase using nocodazole followed by a reversal for 30min. to allow reformation of the spindle and followed by a mitotic shake to release the cells in metaphase. The synchronized cell lysate containing cells at metaphase was passed through a column where the antibody to p(ser9)GSK3β was immobilized on the column. The column was washed to remove unbound components, and then the bound antigen was released into the eluate. Eluates were tested for the presence of the pPKC isoforms as follows. Replicate eluate samples were separated by PAGE (PolyAcrylamide Gel Electrophoresis) and subjected to western blotting using antibodies to different pPKC isoforms to detect a possible association between the inactive GSK3β and pPKC isoforms (Fig. 10a, lanes marked as IP). To control for the detection efficiency and exposure time of the pPKC antibodies, parallel samples of 3T3 cell lysates were subjected to SDS-PAGE, and western blots of the gel were challenged with antibodies to the pPKC isoforms, pPKC α, βII, γ, δ, μ, θ, and ζ (Fig. 10a, lanes marked as CL). The blot shows a binding interaction between the various pPKC isoforms and p(ser9)GSK3β. Phospho-PKCζ had the highest binding with p(ser9)GSK3β. Phospho-PKCδ had detectable binding with p(ser9)GSK3β, while binding of pPKC isoforms α, βII, γ, with p(ser9)GSK3β was not detectable. There was a very low level of binding of p(ser9)GSK3β with

pPKCs μ, and θ. As a control, pPKCζ was immobilized on a column and the column was challenged with the synchronized cell lysate. The column was washed, the bound materials eluted and separated by SDS-PAGE. Western blots of the gel were challenged with antibodies to p(ser9)GSK3β (Fig. 10a far right column) and the band corresponding to p(ser9)GSK3β was detected. The western blot results are shown as a graph depicting the relative intensity of the bands corresponding to each pPKC isotype (Fig. 10b). From the graph in figure 10b it can be seen that the binding of pPKCζ with p(ser9)GSK3β is the strongest followed by pPKCδ. Taken together, the immunocytochemical co-localization, FRET analysis and immunopurification data support the prediction that pPKCζ interacts with GSK3β at the centrosomal region of the mitotic spindle.

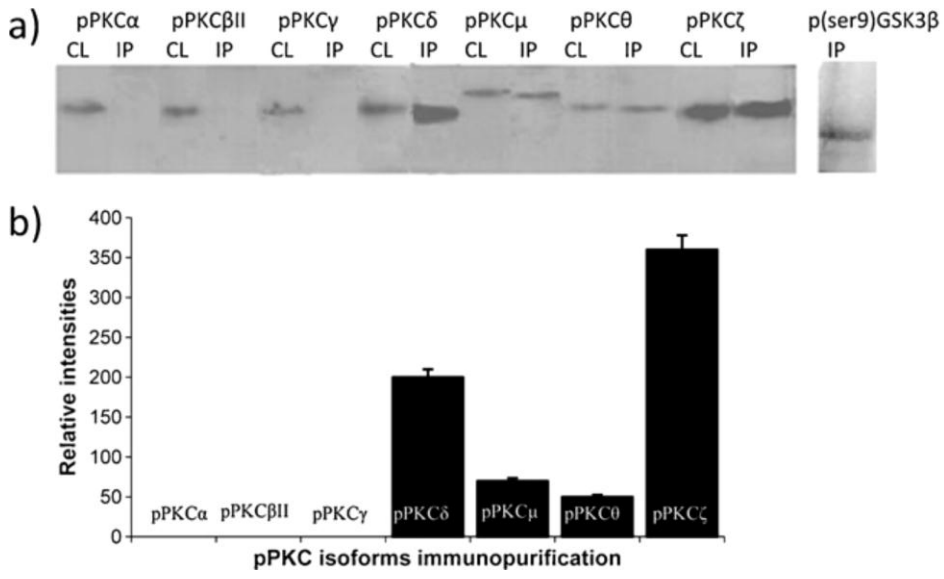

Figure 10. Western analysis of 3T3 cells at metaphase stage to show interaction of pPKC isotypes with p(ser9)GSK3β. (a) The 3T3 cells were synchronized to metaphase and immunopurified (IP) with p(ser9)GSK3β that was immobilized in the column. Antibodies to various phospho isotypes of PKC were used to test the interaction with p(ser9)GSK3β. 3T3 cell lysate samples (CL) were also subjected to SDSPAGE. The Western blots were treated with the pPKC antibodies, used as

controls for detection efficiency of these antibodies. As a control, pPKCζ was immobilized on a column, and the column eluate was challenged with an antibody to p(ser9)GSK3β. This binding of p(ser9)GSK3β with pPKCζ is shown in the lane labeled as pGSK3β which is the far right band in (a). (b) The histogram shows the relative intensity of the bands corresponding to each pPKC isotype. The binding of pPKCζ with p(ser9)GSK3β is the strongest followed by pPKCδ. Equal amounts of protein for each pPKC isoform were loaded on the gel (see "Materials and Methods").

Involvement of inactive GSK3β in maintaining the mitotic spindle

The close proximity and interaction between pPKCζ and p(ser9)GSK3β provides the possibility that pPKCζ can inactivate GSK3β which then results in maintaining the organization of the spindle, (Goold and Gordon-Weeks, 2001; Doble and Woodgett, 2003; Etienne-Manneville and Hall, 2003; Krishnamurthy et al. 2007). To test the importance of inactive GSK3β in maintaining an intact mitotic spindle, a permeabilization experiment was conducted. Mouse fibroblast (3T3) cells were permeabilized by treatment with a mild detergent, Tween-20, using a buffer that mirrors the intercellular environment, along with competitive protease inhibitors (Fig. 11). The permeabilized cells were subjected to a series of treatments detailed below. After these treatments, the cells were cytologically fixed and labeled to view both DNA and α-tubulin, the former to show the organization of the chromosomes and the latter to view the condition of the mitotic spindle. Figure 11a shows the mitotic spindle in an intact cell compared to figure 11b which shows the spindle in an otherwise untreated, permeabilized cell. This shows that permeabilization does not disrupt the spindle or the metaphase plate array of chromosomes. Permeabilized cells treated with active GSK3β kinase for 30min. showed disruption of the spindle microtubule array

(Fig. 11c). There was an average of 70% cells with disrupted spindles and 30% with intact spindles at the 30min. time point. Cells incubated for 1 hour show that the mitotic spindle is virtually absent and the chromosomes begin to diffuse from a distinct metaphase configuration (Fig. 11d). After 1 hour of treatment with the active GSK3β kinase no cells had an intact spindle. In contrast, when active GSK3β was flushed into cells along with an excess of a GSK3β kinase specific peptide inhibitor, the spindle is clearly identifiable though slightly disorganized at the 30min and 1hr time points (Fig. 11e, f). This phenomenon was observed in all the cells scored at metaphase in three independent experiments (fifty cells at metaphase were observed in each experiment). These results indicate that GSK3β needs to be inactivated in order to maintain mitotic spindle organization at metaphase.

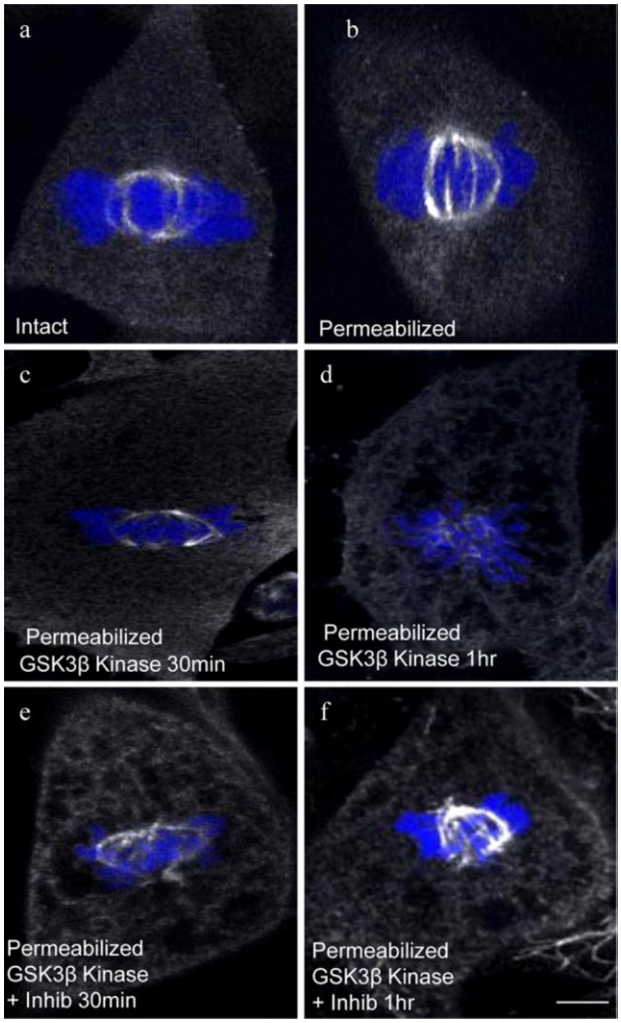

Figure 11. 3T3 cells permeabilized and treated with active GSK3β kinase. (a) An intact cell and (b) permeabilized cell is shown for comparison. Cells were labeled with α-tubulin antibody to identify the spindle (gray). The chromosomes are shown by DRAQ5 staining (blue). (c) Permeabilized cells treated with active GSK3β kinase show spindle disruption at 30min (there were an average of 70%cells with disrupted spindle and 30% with an intact spindle) and (d) increased spindle disruption at 1 h. (e) When the GSK3β pseudosubstrate inhibitor is added with the kinase and applied to permeabilized cells, the spindle structure is maintained after 30 min of treatment and also at (f) 1 h of treatment. The experiment was repeated three times independently, and each time 50 cells at metaphase were scored for spindle condition. Scale bar is10 μm.

pPKCζ inhibitor studies

The prediction that pPKCζ is involved in inactivating GSK3β was further tested by blocking the activity of pPKCζ in living cells with a specific pPKCζ peptide inhibitor. If pPKCζ is responsible for the inactivation of GSK3β then inhibition of pPKCζ should permit activation of GSK3β and consequently the mitotic spindle should become disrupted. This was tested using a myristoylated cell-permeable, peptide inhibitor specific to pPKCζ. The concentration of the pPKCζ inhibitor to be employed and the duration of exposure were determined using a dose response analysis (see Materials and Methods). The inhibitor was added to the medium at a 50μM concentration for an hour. The control cells (without the inhibitor treatment) and the treated cells were double labeled with antibodies to pPKCζ (red) and α-tubulin (green) to visualize pPKCζ and spindle microtubules respectively. The control cells (Fig. 12 panel a, merged image) show a green spindle and yellow centrosomal poles (the contribution of green and red gives yellow when they are co-enriched as seen in the merged image). Cells treated with the pPKCζ inhibitor have no detectable pPKCζ at the centrosome and no detectable spindle microtubules after one hour of incubation in the pPKCζ inhibitor (Fig. 12 panel b). In parallel experiments, cells also were labeled to detect pPKCζ (red) and p(ser9)GSK3β (green). In control cells (without inhibitor treatment) these form the yellow spots representing a co-localization at the centrosome as seen in the merged image (Fig. 12 panel c). In the inhibitor treated cells (Fig. 12 panel d) there is no co-localization of pPKCζ and p(ser9)GSK3β after one hour of incubation in the pPKCζ inhibitor. In order to test if the spindle

microtubules are maintained by inactivating GSK3β, an inhibitor to GSK3β was added to the cells following the addition of pPKCζ inhibitor. The GSK3β inhibitor concentration and incubation time was determined by a dose reponse study as 2.4 μM for 1hr. In figure 12 panel e, it can be seen that the spindle structure is maintained and also the signal for the inactive p(ser9)GSK3β can be detected. In addition, both pPKCζ inhibitor (50μM) and GSK3β inhibitor (2.4μM) were added simultaneously and incubated for 1hr. In figure 12 panel f it can be seen that the metaphase spindle is maintained and looks better than the spindle in figure 12 panel e. The signals for, inactive p(ser9)GSK3β (red) and α-tubulin (green) can be detected in figure 12 panel f. Treatment with the GSK3β inhibitor likely inactivated GSK3β and resulted in stabilization of the spindle in the presence of pPKCζ inhibitor.

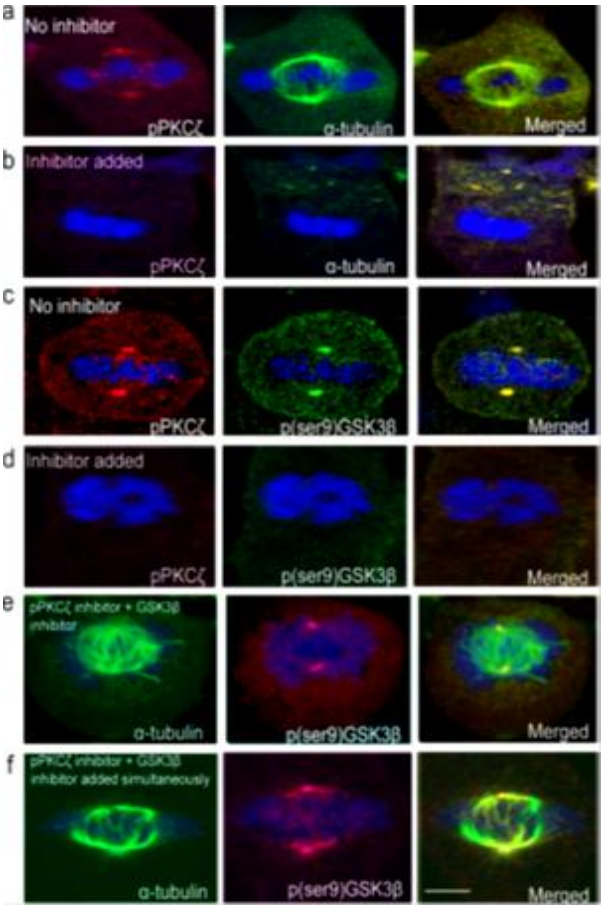

Figure 12. Effect of the inhibition of pPKCζ by a myristoylated pPKCζ peptide-specific inhibitor on α-tubulin and p(ser 9)GSK3β in 3T3 cells. Cells were visualized by immunocytochemistry and confocal microscopy. (a) Control cells not treated with the pPKCζ inhibitor. A control cell (no inhibitor) is shown double-labeled with phospho-PKCζ (red) antibody and α-tubulin antibody (green). The merged image of this labeling is also shown. (b) The experimental cells were treated with 50 μM pPKCζ inhibitor for 1 h. A treated cell is shown double-labeled with phospho-PKCζ (red) antibody and α-tubulin antibody (green), the merged image is also shown. (c) A control cell (no inhibitor) is shown double-labeled with phospho-PKCζ (red) antibody and p(ser9)GSK3β antibody (green) along with the merged image. (d) A treated (50 μM pPKCζ inhibitor for 1 h) cell is shown doublelabeled with p(ser9)GSK3β antibody (green) and with phospho-PKCζ (red) antibody along with the merged image. (e) A cell treated with 50 μM pPKCζ inhibitor for 1 h followed by treatment with 2.5 μM GSK3β inhibitor for 1 h is shown double-labeled with α-tubulin antibody (green) and with p(ser9)GSK3β antibody (red) along with the merged image. (f) A cell treated simultaneously with 50 μM pPKCζ inhibitor and 2.5 μM GSK3β inhibitor for 1 h is shown double-labeled with α-tubulin antibody (green) and with p(ser9)GSK3β

antibody (red) along with the merged image. The chromosomes of the cells are shown in blue. Scale bar is 10 μm.

In order to further study the effects of the pPKCζ inhibitor on p(ser9)GSK3β and pericentrin (a centrosome specific marker), both of which interact with pPKCζ, an immuno-pulldown assay was performed. Cell lysates were prepared from cells that had been treated with the pPKCζ inhibitor for one hour and from control, untreated cells. Prior to preparation of the cell lysates the cells were synchronized into M phase as described in a previous section. The 3T3 cells were treated with 50μM concentration of pPKCζ inhibitor (determined from the dose response analysis) and this cell lysate along with the control cell lysate were applied to separate columns where the antibody to pPKCζ was immobilized. The column was then washed to remove unbound components and the bound antigen was then released into the eluate. Replicate eluate samples were separated by PAGE and subjected to western blotting using antibodies to either pPKCζ, pericentrin or p(ser9)GSK3β. In the western blot (Fig. 13a) cells without the pPKCζ inhibitor are indicated by a '-' on top of the lanes while the cells treated with the pPKCζ inhibitor are indicated by a '+' on top of the lanes. In the blot, the bands in the two left lanes show a reduction in the amount of pPKCζ indicating that the pPKCζ inhibitor did inhibit the activity of pPKCζ in the cellular lysate used. This assay would detect only the level of active kinase and not the total amount of kinase. The amount of pericentrin bound to pPKCζ is greatly reduced in the cell lysates of pPKCζ inhibitor treated cells as compared to the control cell lysate (middle two lanes). The amount of p(ser9)GSK3β bound to

pPKCζ was also reduced in cell lysates of pPKCζ inhibitor treated cells. The results of the western blot are shown as a graph depicting the pixel intensities of the bands on the gel (Fig. 13b).

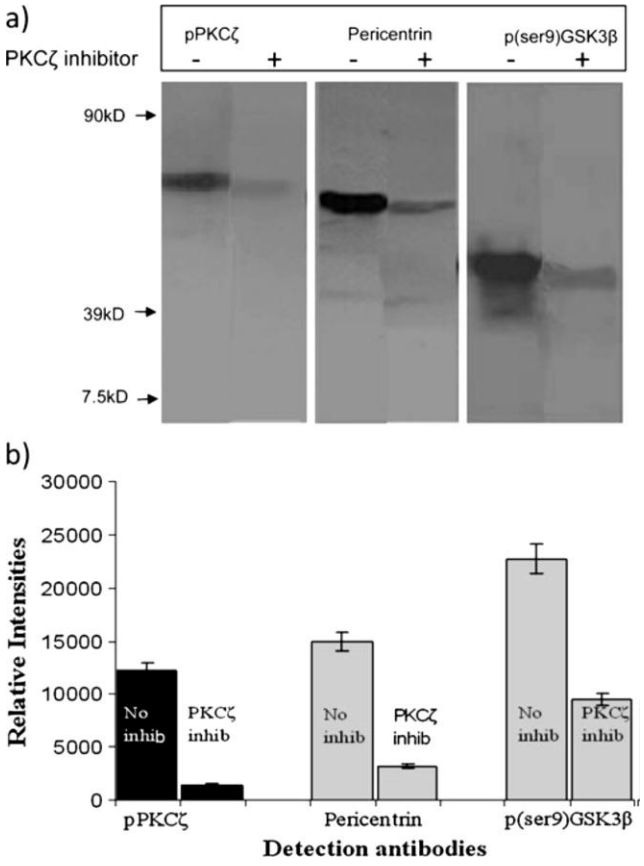

Figure 13. Western analysis of 3T3 cells treated with pPKCζ inhibitor and immunopurified to test the effects of the inhibitor on p(ser9)GSK3β and pericentrin binding. (a) In the Western blot, pPKCζ 'minus sign' and pPKCζ 'plus sign' show the presence or absence of pPKCζ, respectively, in the control cell lysate vs the cell lysate treated with the pPKCζ inhibitor. Pericentrin 'minus sign' and pericentrin 'plus sign' show the binding of pericentrin, a centriolar with pPKCζ in the absence or presence of the pPKCζ inhibitor. In the presence of the inhibitor, there is decreased binding of pericentrin as compared with the control cell lysate. P(ser9)GSK3β 'minus sign' p(ser9)GSK3β 'plus sign' show the binding of p(ser9)GSK3β with pPKCζ in the absence or presence of the pPKCζ inhibitor. In the presence of the inhibitor, there is decreased binding of GSK3β. (b) The histogram shown below compares the relative intensities of the protein bands.

Discussion

PKCs (protein kinases C) are a family of phospholipid-dependent serine/threonine kinases with a central role in signal transduction and regulation of diverse physiological processes, (Durgan et al. 2008; Roffey et al. 2009; Rosse et al. 2010). PKC has been shown to interact with proteins in dynamic cellular compartments including the cytoskeletal network; the latter suggests involvement of PKC in cytoskeletal remodeling, (Jaken and Parker, 2000). The centrosomal spindle which occurs during mitosis has centrioles, and astral microtubules, (Compton, 2000) that form from the centrosome. The "plus" ends of the microtubules extend from the centrosomal region and are captured and stabilized by the kinetochore of the chromosome. This type of spindle assembly is referred to as the "search and capture model" (Holy and Leibler, 1994; Vernos and Karsenti, 1995; Andersen et al. 1997; Huang and Huffaker 2006; O'Connell and Khodjakov, 2007; Przewloka and Glover, 2009). Previous studies have shown association of PKC isoforms at various locations on the mitotic spindle apparatus including PKCβII, PKCε, PKCθ, and PKCζ, (Lehrich and Forrest, 1994; Passalacqua et al. 1999; Chen et al. 2004; Eng et al. 2006; Liu et al. 2006) however there are few details about their function. In addition, glycogen synthase kinase 3β (GSK3β) is a regulator of microtubule stability and active GSK3β disrupts the spindle whereas GSK3β needs to be inactivated to maintain the mitotic spindle, (Wakefield et al. 2006).

Based on these previous studies, we hypothesized that phospho-PKCζ (pPKCζ) interacts with GSK3β to regulate mitotic spindle stability in the metaphase stage of somatic cells with a centrosomal spindle. In this study, the enrichment of the various phosphorylated PKC isoforms in the region of the mitotic spindle, along with their binding with p(ser9)GSK3β has been assessed in the metaphase stage of somatic 3T3 cells, at the centrosome region. The results from this study support our predictions proposed earlier that is, 1) there is significant co-localization and molecular proximity between pPKCζ and inactive GSK3β in the regions of the centrosome and, 2) inhibitors of pPKCζ may act through GSK3β to disrupt the proteins involved in maintaining spindle stability such as p(ser9)GSK3β as well as the spindle structure itself.

In addition, the data resulting from this study indicate that among the phospho PKC isoforms studied, pPKCζ is more likely to be involved in stability of microtubules in the centrosomal mitotic spindle apparatus during cell division in mouse cells. The mitotic cells employed in this study, 3T3 mouse fibroblasts, represent an immortal cell line, however they are anchorage-dependent for growth as normal fibroblast would be, and more to the point, do undergo mitosis with a centrosomal spindle.

Protein kinase C (PKC) isoforms in the spindle apparatus of somatic cells

In this study, the atypical isoform PKCζ in its phosphorylated form was enriched at the centrosome of intact cells at significantly higher levels than the

other pPKC isoforms tested except pPKCδ as determined by the pixel intensity ratio analysis. Detergent extraction studies showed that pPKCζ is part of the spindle scaffold. Interestingly, pPKCζ was also enriched at the chromosomal region of metaphase 3T3 cells. None of the other pPKC isoforms tested showed enrichment at the chromosomal region of metaphase cells. In an earlier study, pPKCζ was shown to be associated with the kinetochore region of 3T3 cells, (Liu et al. 2006). It is possible that pPKCζ is associated with the kinetochore region in the current study.

PKC isoforms and GSK3β

In this study, p(ser9)GSK3β was found enriched at the centrosomes in the metaphase stage of 3T3 mouse fibroblasts. Phospho-PKCζ and pPKCδ co-localize with p(ser9)GSK3β at the centrosomes. Frame averaging of the confocal images showed that pPKCζ also co-localizes with pGSK3β in the chromosomal region.

FRET (fluorescent resonance energy transfer) is a useful method to determine close proximity between proteins. A FRET value can be measured only if the fluorescent emitting molecules are within a proximity of 10-100 Å. If pPKC isoforms and GSK3β interact, the proteins should be in close molecular proximity for some time in a metaphase cell. FRET was used to measure the potential energy transfer between the pPKC isoforms tested and p(ser9)GSK3β at the centrosomes and the kinetochore region. There was significant energy transfer between pPKCζ and p(ser9)GSK3β with an average value of 33.51% at

the centrosome and an average value of 47.2% at the kinetochore region. FRET was detected between pPKCζ and pericentrin at the centrosome with a value of 5%, also a FRET value of 8% was detected between γ-tubulin and pPKCζ at the centrosome. This confirms that pPKCζ is in close association with key elements (i.e. pericentrin and γ-tubulin) of the centrosome region. The value for the energy transfer between pPKCδ and p(ser9)GSK3β was an average of 4.56% at the centrosome and an average of 5.27% at the chromosomal region, which is lower than the values for pPKCζ. FRET was absent for the other isoforms tested in this study. Thus, at both the centromere and chromosomal region there is close molecular proximity between pPKCζ and p(ser9)GSK3β and to a lesser extent between pPKCδ and p(ser9)GSK3β as seen from the FRET and western blot data.

Taken together, the results from co-localization studies and FRET analyses support our prediction that there should be significant co-localization and molecular proximity between pPKCζ and inactive GSK3β in the regions of the centrosome and the chromosomal region.

Functional significance of PKCζ and GSK3β in the mitotic spindle

The close proximity of the active form of PKCζ to GSK3β suggests that it may inactivate GSK3β by phosphorylating on the ser9 residue on GSK3β at the centrosome region. GSK3β is a complex kinase that becomes inactive when phosphorylated on ser9 by pPKCζ, (Frame and Cohen, 2001; Krishnamurthy et al. 2007) and inactivation of GSK3β has been shown to facilitate microtubule

stability. We hypothesized that pPKCζ interacts with GSK3β to regulate spindle structure. In order to test the importance of inactive GSK3β to maintain the mitotic spindle, active GSK3β was added to permeabilized 3T3 cells, which resulted in the disruption of the spindle apparatus. On the other hand, addition of active GSK3β along with a GSK3β inhibitor resulted in stabilization of the spindle. The latter result suggested that inactivation of GSK3β is necessary for maintenance of the mitotic spindle. When GSK3β is phosphorylated, it results in dephosphorylation of known microtubule binding proteins (MBPs) like CRMP-2 and APC thus leading to microtubule stabilization, (Zhou and Snider, 2005; Yoshimura et al. 2005). In its active form, GSK3β activates via phosphorylation, targets such as Microtubule Associated Protein 1B (MAP1B), Tau and EB1 which destabilize microtubules and maintain them in a dynamic state, (Liu et al. 2003; Goold and Gordon-Weeks 2004; Trivedi et al. 2005; Vaughn, 2005).

The addition of a specific inhibitor to pPKCζ likely causes decreased levels of inactive GSK3β in 3T3 cells at metaphase and results in the disruption of the mitotic spindle as seen from the immunocytochemical and the western blot results. This supports our second prediction that inhibitors of pPKCζ may act through GSK3β to disrupt the proteins involved in maintaining spindle structure. However it is worth noting that it has been shown earlier that at micromolar concentrations (1–10 μM), the pseudosubstrate inhibitor to PKCζ can induced phosphorylation of eNOS, Akt, ERK 1/2, and p38 MAPK in cultured pulmonary artery endothelial cells (PAEC), (Krotova et al. 2006). In the NIH 3T3 cells used in this study, it may be possible that these other pathways have an influence on

the interaction between pPKCζ and GSK3β. Mitotic spindle structure disruption by the addition of pPKCζ inhibitor can be reversed by addition of GSK3β inhibitor, which is further evidence that spindle structure maintenance, may occur by the inactivation of GSK3β. Also, when both pPKCζ inhibitor and GSK3β inhibitor were added simultaneously, the GSK3β inhibitor may have stopped spindle from disrupting which would have occurred in the presence of pPKCζ inhibitor alone thus retaining the spindle.

Although little is known about their function, many of the PKC isoforms have been shown to be present in the acentrosomal spindle apparatus of the mouse egg, (Gangeswaran and Jones, 1997; Raz et al. 1998; Pauken and Capco, 2000; Viveiros et al. 2001; Baluch and Capco, 2002; Viveiros et al. 2003; Baluch et al. 2004; Kalive et al. 2009) and these related studies show some notable differences when compared to mouse fibroblasts (mitotic cells). In the mouse egg, which has an acentrosomal spindle, pPKCζ is present as a ring at the end of each spindle pole whereas the somatic cells have a distinct spot that overlaps the centrosome. This difference may result because meiotic cells have a barrel-shaped spindle and PKCζ may be lining the edge of the barrel-shaped spindle, whereas in the mitotic cells, all the spindle microtubules end at the centrosome. In meiotic eggs, pPKCζ may have a role in stabilizing the ends of the barrel shaped spindle in the absence of centrioles, (Baluch and Capco, 2008). Another notable difference between meiotic and mitotic cells is that pPKCγ localizes as a distinct spot at the end of the spindle in meiotic cells, whereas in mitotic cells pPKCγ appears to line the

spindle microtubules which is also seen when the mitotic cells are subjected to detergent extraction.

The assembly of the mitotic spindle is not similar to the assembly of the meiotic spindle. The mitotic spindle assembles by "search and capture" while the meiotic spindle assembles by molecular motors that move and bundle microtubules at their minus ends, (Karsenti and Vernos, 2001; Huang and Huffaker, 2006; O'Connell and Khodjakov, 2007; Przewloka and Glover, 2009). It is interesting to note that both pPKCζ and p(ser9)GSK3β are present at the chromosomal region in the metaphase stage. This possible interaction may be important to stabilize the astral microtubules when they "capture" the kinetochore region. It will be important to study if GSK3β is phosphorylated by pPKCζ in the anaphase and telophase stages following metaphase and if this interaction is required to stabilize the microtubules in those stages also especially in the telophase stage when each daughter cell has one centrosomal region. At these later stages, it can be speculated that an alternate pPKC isoform such as pPKCδ may also interact with GSK3β to stabilize the microtubules as a "back-up" to pPKCζ or the microtubules could be stabilized by other regulatory proteins.

The various PKC isotypes tested have different substrate specificities and may have different roles to perform in the 3T3 cell cycle since all of them are enriched at the centrosome and have varying requirements for activation. The mitotic spindle itself may serve as a scaffold to hold all these elements along with the other elements involved in the cell cycle machinery.

Chapter 3

INVOLVEMENT OF MEK, ERK, PKCZETA AND GSK3BETA IN MAINTAINING THE MITOTIC SPINDLE

Madhavi Kalive, David G. Capco

Introduction

The MAPK pathway is involved in a multitude of functions including cell cycle regulation, cell differentiation, and cell death in eukaryotes ranging from yeast to humans (Nigg et al. 2001; Orton et al. 2005; Rozengurt, 2007; Marks et al. 2009). As part of this pathway, many somatic cell studies have shown that Raf kinase activates MEK1/2 (MEK) by phosphorylation of two serine residues. MEKs generally recognize only specific MAPKs as substrates. It has been reported that MEK phosphorylates ERK 1/2 (ERK) at threonine and tyrosine residues in a 'TEY' motif within its activation loop (Yung et al. 1997, Orton et al. 2005).

In mammalian mitosis, the MAPK pathway in has been extensively examined. For example studies indicate that activation of the MEK/ERK pathway is required for normal progression into mitosis (Guadagno and Ferrell, 1998; Wright et al. 1999; Hayne et al. 2000). In somatic cells such as the 3T3 cells used in this study, the mitotic spindle is centrosomal and a dynamic structure that facilitates chromosome segregation. Many studies have observed that the mitotic spindle apparatus is composed of several elements including centrosomes, microtubules such as astral, polar, and kinetochore microtubules, kinetochores of

chromosomes, and associated proteins (McIntosh and Landis, 1971; Burbank et al. 2007; Walczak and Heald, 2008; Schmidt et al. 2010). It has been reported that activated MEK and ERK localize to the centrosomes of the mitotic spindle from prophase to anaphase, and to the midbody during cytokinesis (Shapiro et al. 1998; Willard and Crouch, 2001; Collelo et al. 2012). ERK, the known downstream target of MEK has been shown to be associated with the centrosome and kinetochore components of the mitotic spindle apparatus, and has multiple functions during mitosis including, promoting mitotic entry as well as targeting proteins that mediate mitotic progression in response to kinetochore attachment (Schmidt-Alliana et al. 1998; Shapiro et al. 1998; Saffery et al. 2000). Activated ERK co-localizes with the kinetochore motor protein CENP-E, raising the possibility that CENP-E is a downstream effector for ERK during mitosis (Zecevic et al. 1998; Willard and Crouch, 2001; Chambard et al. 2006). Studies have shown that blocking MEK activity in cycling somatic cells does not significantly affect mitotic entry, but it does slow progression through mitosis, probably by slowing the CENP-E-dependent chromosome movements coordinated by the mitotic spindle (Roberts et al. 2002). Other studies have shown that active MEK along with active cyclinB-Cdc2 is necessary for the cells to progress into M-phase (Harding et al. 2003; Walsh et al. 2003).

Signaling networks are important for cell proliferation, and communication between pathways can take place at many locations from the plasma membrane to the nucleus. MAPK pathways cross-communicate with other signaling pathways such as the GSK3 pathway and the PKC pathway (Nigg,

2001; Zhang and Liu, 2002; Kholodenko, 2006; Rozengurt, 2007). Glycogen synthase kinase 3β (GSK3β) and protein kinase C (PKC) have been found to be associated with the mitotic spindle (Lehrich and Forrest, 1994; Etienne-Manneville and Hall, 2003; Wakefield et al. 2003; Jope and Johnson, 2004; Liu et al. 2006; Kalive et al. 2011). Earlier studies have shown that GSK3β is associated with the centrosome and is known to phosphorylate microtubule associated proteins (MAPs) such as MAP1B which in turn causes chromosomal segregation by the microtubules. In these studies the MAPK pathway was shown to be upstream of GSK3β (Goold et al. 1999; Frame and Cohen, 2001; Goold et al. 2005; Scales et al. 2009).

PKCs also have been reported previously as upstream activators of the MEK/ERK pathway (Brändlin et al. 2002; Puente et al. 2006; Chang et al. 2008; Marks et al. 2009). In an earlier study the PKCζ isoform has been implicated to be an upstream activator of MEK (Berra et al. 1995; Short et al. 2006). In addition, the PKCζ isoform has been shown to be associated with the centrosome region of the mitotic spindle, or with the spindle microtubules (Lehrich and Forrest, 1994; Liu et al. 2006), and its activation is known to play an important role in stable kinetochore-microtubule attachment and subsequent chromosomal separation (Liu et al. 2006). PKC isoforms can directly regulate Raf-1 which is an upstream activator of the MEK/ERK pathway, specifically PKCα and PKCη are known activators of Raf-1 (Schonwasser et al. 1998; Corbit et al. 2003). A previous study showed that inhibition of active PKCζ by a myristoylated peptide inhibitor causes an inhibition of p(ser9)GSK3β at the centrosomes and causes a

disruption of the mitotic spindle. This study also suggests that p(ser9)GSK3β could be a substrate of active PKCζ (Kalive et al. 2011). However, no single study has examined all four of the kinases at the same time in the same cell type.

Taken together these studies indicate that MEK, ERK, PKCζ, and GSK3β can all be important kinases involved with the mitotic spindle and its regulation. However from these previous studies it is not clear if these kinases are part of a single signaling pathway that regulate the mitotic spindle apparatus or whether there are multiple pathways engaged in cross-talk between the pathways.

In this study, MEK and ERK activity were separately inhibited in the same cell type and it was determined whether this inhibition affects the location and activity of PKCζ and GSK3β. If MEK/ERK, PKCζ, and GSK3β interact then we predicted that they would co-localize at the spindle during mitosis. Moreover, if MEK and ERK have sole control over the mitotic spindle then inactivation of either MEK or ERK may obliterate the spindle and progression through mitosis. In contrast, if multiple signaling pathways are involved then a modification or reduction in the spindle might be observed and only a reduction in the progression through mitosis.

Materials and Methods

Cell culture and media

The cells used for all the experiments were NIH 3T3 mouse fibroblasts, ATCC number CRL-2795. Cells were maintained at 10% CO_2 concentration in a 37°C moisture incubator. Dulbecco's Modified Eagle's Medium (DMEM) was used to maintain the cells (10% calf serum, 1% penicillin–streptomycin, 2% L-glutamine). The cells were grown to 80% confluency before being used. All chemicals used in experiments were obtained from Sigma (St. Louis, MO USA) unless otherwise indicated.

Inhibitor treatment: MEK siRNA, U0126, ERK activation peptide inhibitor

A dose–response analysis was performed in order to determine the amount of inhibitor to be added to the cells, and the time of exposure.

MEK siRNA: 3T3 cells were exposed to increasing concentrations of the inhibitor according to the protocol provided by the manufacturer (Santa Cruz Biotechnology, Santa Cruz, CA USA). Briefly, MEK siRNA at concentrations of 1µM, 5µM, 10µM, and 20µM were introduced into cells using the reagents supplied by the manufacturer. After 48hrs cells were subjected to immunocytochemical analysis using the pMEK specific antibody, and then viewed by confocal microscopy. The optimal concentration of the MEK siRNA inhibitor i.e. the lowest possible concentration that completely suppressed pMEK was determined as 10µM and was used at this concentration for the studies performed.

U0126 inhibitor: 3T3 cells were exposed to increasing concentrations of the inhibitor (Calbiochem, La Jolla, CA USA) at 10µM, 25µM, 100µM, and 150µM in DMEM media for 5.5h, then subjected to immunocytochemical analysis using the pMEK specific antibody and viewed by confocal microscopy. The optimal concentration of the inhibitor was determined as 100µM which was the lowest possible concentration that completely suppressed pMEK. MEK inhibitor U0126 was used at 100µM for 5.5h for the studies performed.

ERK activation peptide inhibitor: 3T3 cells were exposed to increasing concentrations of the peptide inhibitor (Calbiochem, La Jolla, CA USA) such as 10µM, 25µM, 100µM, and 150µM in DMEM media for 4h, then subjected to immunocytochemical analysis using the pERK specific antibody and viewed by confocal microscopy. The optimal concentration of the inhibitor was determined as 100µM which was the lowest possible concentration that completely suppressed pERK. ERK inhibitor was used at 100µM for 4h for the studies performed.

Immunocytochemistry

The living 3T3 mouse fibroblast cells were fixed intact for 30 min in 2% formaldehyde in ICB (ICB-100 mM KCl, 5 mM MgCl2, 3 mM EGTA, and 20 mM HEPES (pH 6.8), in H2O) and permeabilized for 1 h in ICB with 2% paraformaldehyde and 1% Tween-20. The samples were then washed three times for 15 min, each wash with ICB-bovine serum albumin (BSA) buffer (1% BSA in ICB). In separate experiments primary antibodies were then added to the cells in

the antibody dilution buffer (1% nonfat milk, 0.5% Tween-20 in ICB) at a 1:500 dilution for each antibody, overnight at 4°C with gentle rocking. The following day, the cells were washed with the ICB-BSA buffer three times, at 15 min each wash with gentle rocking. The appropriate secondary antibodies were added to the cells overnight at 4°C with gentle rocking. The secondary antibodies were made in the antibody dilution buffer at a 1:1,000 antibody concentration. The following day, cells were washed with the ICB-BSA buffer three times, at 15 min each wash, and then placed in DRAQ5 (2.4 μg/mL in ICB [Axxora, LLC]) for a 15-min incubation. This was done to visualize the chromosomes in the confocal microscope. The primary antibodies used were: anti-pMEK, anti-tMEK, anti-pPKC ζ (Santa Cruz Biotechnology, Santa Cruz, CA), anti-pERK, anti-tERK, anti-p(ser9) GSK3β (Cell Signaling Technology, Beverly, MA USA), anti-α-tubulin (Sigma Aldrich, St. Louis, MO USA), anti-γ-tubulin (Sigma Aldrich, St. Louis, MO USA). The secondary antibodies used were Alexa-568- and Alexa-488-conjugated IgGs (Molecular Probes Inc, Eugene, OR USA). All experiments were performed in triplicate independently.

Confocal microscopy

The cells were mounted on coverslips sealed with nail polish after the immunocytochemistry procedure. The cells were viewed on the Leica SP2 microscope in the W. M. Keck Bioimaging Laboratory at Arizona State University. Multiple lasers allowed for simultaneous imaging of the Alexa 488 and Alexa 568 (argon 488 nm; krypton 568 nm) fluorophore-labeled samples.

Using a 100x oil objective, images were scanned at 0.5μM slices in the Z-axis at the spindle region. The image files were analyzed using the Leica NTS software (Leica Microsystems, Bannockburn, IL USA).

Cell cycle quantification

3T3 cells were treated with MEK siRNA, U0126, ERK activation peptide inhibitor or left untreated as control cells in separate experiments. After performing the immunocytochemistry procedure, cells were labeled with an antibody against α-tubulin. The chromosomes were visualized by staining with DRAQ1 (2.4 μg/mL in ICB [AXXORA, LLC]). The cells viewed by confocal microscope were divided into quadrants and a total of about four thousand cells were analyzed. The number of cells in the cell cycle stages such as, pre-metaphase (stages earlier than metaphase), metaphase, anaphase, telophase, and cytokinesis were counted within each of the quadrants. This was repeated for all the treatments studied. Every treatment experiment was performed in triplicate, the numbers of cells in each cell cycle stage were counted, an average calculated along with the standard error of the mean and the averages were converted to percentages. This data was then represented graphically with the cell cycle stages on the X-axis and the percentage numbers of cells in each cell cycle stage on the Y-axis. Statistical significance was calculated by comparing the control values versus experimental values using a Student t-test and a probability of $p<0.05$ was considered as significant. All experiments were performed in triplicate independently

Transfection with MEK plasmid

MEK plasmid was transiently transfected into 3T3 cells according to the protocol by Life technologies Inc. using Lipofectamine™ 2000 (Life technologies Inc, Carlsbad, CA USA). Briefly, cells were grown in 60mm petri-dishes until 70% confluent. Twenty-four hours after transfection fresh media was added to the cells and after 48h of transfection cells were used for further analyses. The same protocol was followed when cells were transiently transfected with a combination of MEK plasmid and MEK siRNA.

RNA isolation and RT-PCR

3T3 cells were grown in 60mm petri-dishes until they were 70% confluent. The total RNA from each of the petri-dishes was isolated after 48hrs of treatment, then reverse transcriptase (RT) reaction was conducted to isolate the cDNA from each treatment category. RNA easy mini kit (Qiagen, Maryland USA) was used to isolate the RNA. The isolated cDNA was then subjected to PCR (polymerase chain reaction). The primers used for the PCR reactions were, forward and reverse primers for MEK (Santa Cruz Biotechnology, CA) and the forward and reverse primers for GAPDH (glyceraldehyde 3-phosphate dehydrogenase) (Santa Cruz biotechnology). The RT-PCR products were run on a 1% agarose gel along with the 1kb DNA ladder as a molecular weight marker. All experiments were performed in triplicate independently.

Immunoblotting

A Bradford assay was performed in order to determine the concentration of protein that was loaded onto the SDS gel. The samples used for immunoblotting were loaded at a concentration of 750 μg/ml in each lane, to perform SDS-PAGE. Laemmli 2× sample buffer was added to the samples (Laemmli, 1970). The samples were placed in a boiling water bath for 10 min to denature the proteins. The samples were then loaded onto a pre-cast 10% Tris–HCl precise protein gel (Pierce Biotechnology, Rockford, IL USA), and then transferred to a PVDF membrane (Towbin et al. 1979). The Kaleidoscope protein dye was used as the marker to confirm molecular weight. The blot was blocked in BLOTTO, (5% percent non-fat dried milk in PBS-T [PBS with 0.1% Tween-20]) for 1 h; the blot was rinsed and treated with the appropriate primary antibodies at a 1:500 concentration overnight at 4°C. The blot was then washed three times with PBS-T the following day. The appropriate horseradish peroxidase (HRP) conjugated secondary antibody (Pierce Biotechnology, Rockford, IL USA) was applied to the blot as secondary antibody in BLOTTO for 2 h at room temperature. After washing the blot with PBS-T three times, chemiluminescence was used to detect the protein bands on the blot. The ECL plus kit (formerly Amersham Biosciences, Arlington, IL) and the Hyperfilm ECL chemiluminescent film (GE Healthcare, Arlington, IL) were used for the detection. The protein bands from the blots were quantified by calculating the average pixel intensities of the each protein band from three independent experiments and plotting them as a histogram. Image J software was used to calculate the relative band intensity of

the protein bands. Statistical significance was calculated by comparing the control values versus experimental values using a Student t-test and a probability of $p<0.05$ was considered as significant.

Results

Effects of inhibitors of MEK on the co-localization of pMEK with pPKCζ and with p(ser9)GSK3β

The effects of MEK inhibitors on the co-localization of pMEK with pPKCζ and p(ser9)GSK3β at the metaphase stage of 3T3 cells were tested with 2 types of treatments compared to the control cells (no treatment). The treatments applied in parallel were: 1) Cells treated with the MEK small inhibitor RNA (MEK siRNA); and 2) Cells treated with the MEK chemical inhibitor, U0126. The concentration of MEK siRNA and U0126, and the duration of exposure were determined using a dose response analysis (see Materials and Methods). All the cells in culture dishes analyzed were in metaphase. In all figures, the chromosomes can be visualized as blue as a result of labeling with DRAQ5. In control cells (Fig. 14 a, b, and c), the enrichment of pMEK and p(ser9)GSK3β was assessed by labeling the cells both with a pMEK specific antibody (binds to active MEK) and p(ser9)GSK3β specific antibody (binds to inactive (ser9)GSK3β). The enrichment of pMEK was visualized as red in the centrosomal areas on either end of the metaphase plate (indicated by arrows in figure 14a), and the enrichment of p(ser9)GSK3β was visualized as green in the centrosomal areas on either end of the metaphase plate in figure 14b, thus co-localization between

the two appears as yellow spots at the centrosomal areas on either end of the metaphase plate, in the merged image in figure 14c. In order to confirm that the spots on either end of the metaphase plate chromosomes were centrosomes, cells were co-labeled with a centrosomal marker, γ-tubulin (Habermann and Lange, 2012), along with pMEK. The inset in figure 14c indicates a representative metaphase cell co-labeled with antibodies to pMEK (red) and γ-tubulin (green) so that the co-localization at the centrosomes is visualized as yellow. In earlier studies, pPKCζ has been shown to be localized to the centrosomes of the mitotic spindle (Lehrich and Forrest, 1994; Liu et al., 2006). To test if pPKCζ co-localized with pMEK, the enrichment of pMEK and pPKCζ was assessed next in control cells by labeling the cells with a pMEK specific antibody (red) and pPKCζ specific antibody (green) (Fig. 14d, e, and f). Co-localization between the two appears yellow at the centrosomal areas in the merged image in figure 14f.

In cells treated with the MEK siRNA, the effects of inhibiting MEK on p(ser9)GSK3β was demonstrated by labeling the cells with a pMEK specific antibody (red) and a p(ser9)GSK3β specific antibody (green). In figure 14g, there is an absence of pMEK in the centrosomal areas. Phospho(ser9)GSK3β (green) can be visualized in the centrosomal areas in figure 14h. Note the absence of yellow spots at the centrosomal areas that would otherwise indicate the co-localization between the two kinases in the merged image in figure 14i (indicated by arrows). The inset in figure 14i indicates a metaphase cell labeled with antibodies against γ-tubulin (green) at the centrosomes. In MEK siRNA treated cells, the effects of inhibiting MEK on pPKCζ was demonstrated next by labeling

the cells with a pMEK specific antibody (red) and a pPKCζ specific antibody (green). In figure 14j, there is an absence of pMEK in the centrosomal areas. PhosphoPKCζ (green) can be visualized in the centrosomal areas in figure 14k. Note the absence of yellow spots at the centrosomal areas in the merged image in figure 14l (indicated by arrows).

MEK was also inhibited by a different method that is, using a pharmacological inhibitor of MEK to test if the same results were observed. Cells were treated with the pharmacological inhibitor against MEK, U0126 which has been shown to inhibit MEK1 and MEK2 by non-competitive inhibition (Duncia et al., 1998; Favata et al., 1998) and cells were treated with U0126. In the U0126 inhibitor treated cells, the effects of inhibiting MEK on p(ser9)GSK3β was assessed by labeling the cells with a pMEK specific antibody (red) and a p(ser9)GSK3β specific antibody (green). In figure 14m, there is an absence of red pMEK in the centrosomal areas of the cell, while green p(ser9)GSK3β can be visualized in the centrosomal areas (Fig. 14n). A co-localization between the two kinases in the merged image in figure 14o (indicated by arrows) is absent. The inset in figure 14o indicates a metaphase cell showing γ-tubulin (gree en) at the centrosomes. In U0126 inhibitor treated cells, the effects of MEK inhibition on pPKCζ was assessed next by labeling the cells with a pMEK specific antibody (red) and a pPKCζ specific antibody (green). The inhibitor blocked pMEK (Fig. 14p seen as an absence of red), but pPKCζ (green) is present and is shown in the merged image in figure 14r (indicated by arrows).

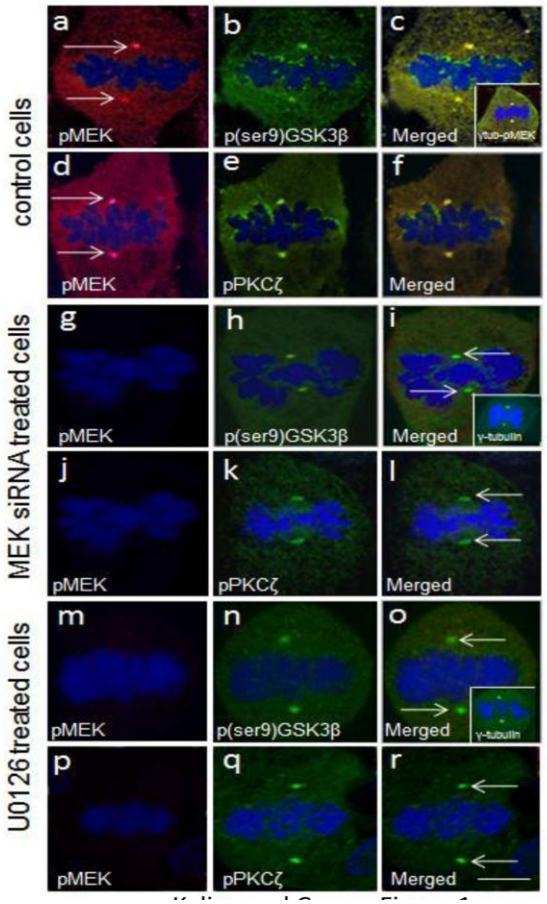

Figure 14: Effect of MEK inhibition on the co-localization of pMEK with p(ser9)GSK3β and pPKCζ in 3T3 cells. (a) In control cells pMEK (red) was tested for co-localization with (b) p(ser9)GSK3β (green) by immunocytochemistry and confocal microscopy. (c) The co-localization of pMEK and p(ser9)GSK3β can be visualized in a merged image with the co-localized areas showing yellow pixels. The arrows in (a) indicate the enrichment of pMEK at the centrosome regions. The inset in (c) is a merged image of a control cell to show the co-localization of pMEK and γ-tubulin at the centrosomes. (d) In control cells pMEK (red) was tested for co-localization with (e) pPKCζ (green) and in the merged image (f) is yellow. (g) In MEK siRNA treated cells, pMEK is absent and there is no co-localization with (h) p(ser9)GSK3β (green). Thus (i) in the merged image the centrosomes are green since there is no co-localization. The arrows in (i) indicate the green pixels at the centrosomes. The inset in (i) is an image of a MEK siRNA treated cell that shows the enrichment of γ-tubulin at the centrosomes. (j) In MEK siRNA treated cells, pMEK (red) is absent, while (k) pPKCζ (green) is present. Thus (l) in the merged image the centrosomes are green since there is no co-localization and this is indicated by arrows. (m,n) In U0126 treated cells, there is an absence of pMEK (red) while p(ser9)GSK3β (green) is present. In the merged image (o) there are green pixels at the centrosomes indicated by arrows. The inset in (o) shows γ-tubulin at the

centrosomes. (p,q) In U0126 treated cells, there is an absence of pMEK (red) while pPKCζ (green) is present. In the merged image (r) centrosomes are green indicated by arrows. All experiments were performed in triplicate. Scale bar is 10μm.

Effects of MEK inhibition on protein expression

A biochemical confirmation of the results from the immunocytochemical co-localization experiments in the previous section, shows the effect of MEK inhibition on cellular protein expression of pMEK, p(ser9)GSK3β and pPKCζ (Fig 15). Cell lysates were prepared from both the inhibitor treatments as well as the control cells and then subjected to immunoblotting. All the blots in figure 15 were also treated with an antibody against Myosin-1 (200kD molecular weight) as a loading control to correct for loading errors (see Materials and Methods). Cells treated with inhibitors of MEK activity were first assessed to determine the effects on total MEK (Fig. 15a) and pMEK (Fig. 15b). The signal for both of these was absent though clearly visible in control cells and also the DMSO carrier control. This was observed for both MEK siRNA and U0126 treated cells (Fig. 15a-b).

Phospho(ser9)GSK3β antibody was used next to detect protein expression of p(ser9)GSK3β in the control lysate along with the U0126 and MEK siRNA treated lysates (Fig. 15c). The expression of p(ser9)GSK3β was detected by a band at the 42kD molecular weight in the control lysate along with the U0126 and the MEK siRNA treated cell lysates. These results support the confocal microscopy images seen in figures 1g, h, i, m, n, and o where p(ser9)GSK3β protein expression was not inhibited by MEK inhibitors, although there was a

significant reduction in the total cellular protein levels of p(ser9)GSK3β after addition of the MEK inhibitors. This protein reduction is seen in the graphical representation of the average protein band intensity from the blots (Fig. 15h). The band intensities for each blot were calculated as an average from three independent experiments and statistical significance was also calculated (see Materials and Methods).

In figure 15d, pPKCζ antibody was used and pPKCζ expression was detected in the control lysate, also in the U0126 treated lysate and the MEK siRNA cell lysate as the 71kD molecular weight band. These results support the confocal microscopy images seen in figures 15j, k, l, p, q and r where pPKCζ protein expression was not inhibited by MEK inhibitors, although there was a significant reduction in the total cellular protein levels of pPKCζ as seen in figure 15h.

To test the effects of MEK inhibition on the mitotic spindle microtubules, the protein levels of α-tubulin were examined. In figure 15e, the α-tubulin antibody was used and α-tubulin expression was detected in the control lysate, also in the U0126 treated lysate and the MEK siRNA cell lysate as a 55kD molecular weight band. There was a significant reduction in the total protein levels of α-tubulin as seen in figure 15h.

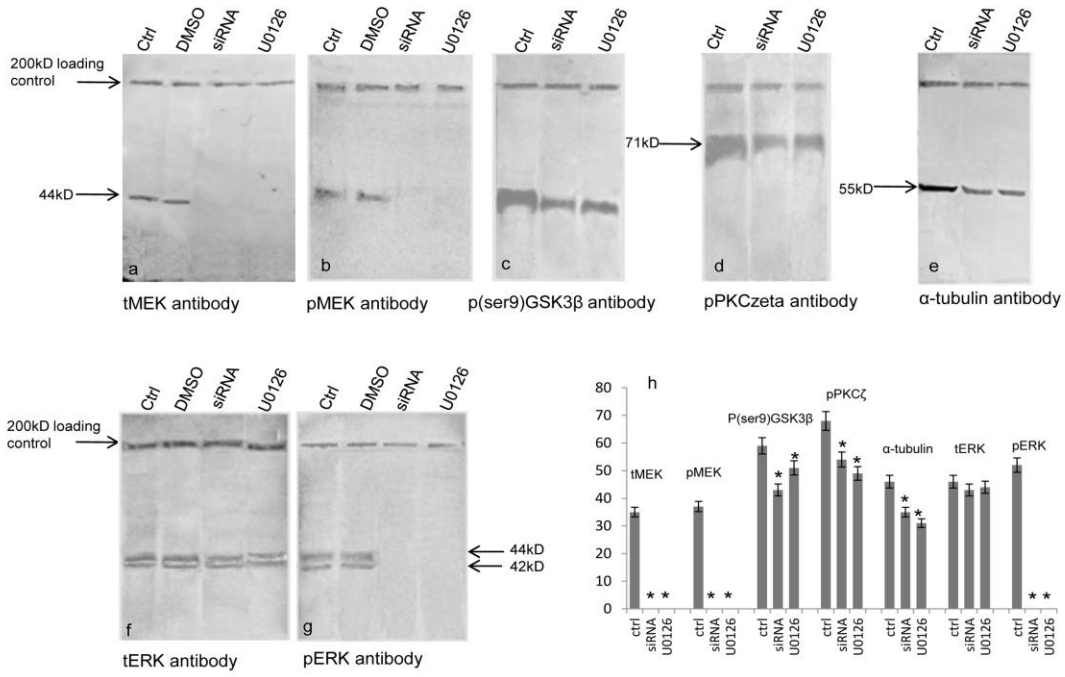

Figure 15: Western analysis of MEK inhibited cell lysates. Control cells have been labeled 'ctrl' and 'DMSO' (for the carrier control) in all the blots of this figure. (a) An antibody to tMEK was used to detect tMEK protein in lysates from control cells, along with lysates from MEK siRNA treated cells and U0126 treated cells. Myosin-1 was used as the loading control with a molecular weight of 200kD in all the Western blots shown in this figure. (b) PhosphoMEK antibody was used to detect cellular protein levels of pMEK in control cells versus MEK siRNA treated cells and U0126 treated cells. Antibodies including (c) p(ser9)GSK3β antibody, (d) pPKCζ antibody, (e) α-tubulin antibody, (f) tERK antibody, and (g) pERK antibody were employed to detect the corresponding cellular protein levels in control cells versus MEK inhibited cells, inhibited by MEK siRNA and U0126. The histogram in (h) represents a quantification of the protein bands seen in the Western blots. The asterisks represent a significant difference from the control lysates. Experiments were performed in triplicate and statistical significance was calculated by a Student t-test and a probability of $p<0.05$ was considered as significant. There is a slight reduction of p(ser9)GSK3β, pPKCζ and α-tubulin protein levels. Equal amounts of each protein were loaded on the gels (see Materials and Methods).

ERK is a known downstream target of MEK in the MAPK pathway of somatic cells (Pumiglia and Decker, 1997; Zhang and Liu, 2002; Orton et al.,

2005; Shaul and Seger, 2007; Borysova et al., 2008). The protein expression pattern of total ERK1/2 (tERK) in the cell population was examined next (Fig. 15f). After immunoblotting, an antibody against tERK1/2 protein was used and the expression of tERK1/2 was visualized as two protein bands at the molecular weights of 44kD and 42kD. The inhibitors, U0126 and MEK siRNA did not affect tERK1/2 protein levels since tERK1/2 was expressed in all of the treatments as seen in the blot and in the graph (Fig. 15h). However when an antibody against phospho ERK1/2 (pERK1/2) was used to test the expression of the active phosphorylated form of ERK1/2 (Fig. 15g), compared to the control cell lysate, pERK1/2 was not expressed in the U0126 and MEK siRNA treated cell lysates since the upstream effector pMEK was inhibited.

Confirmation of MEK siRNA specificity; Effect of MEK overexpression

In order to confirm that MEK siRNA did inhibit the expression of MEK, experiments were performed with a MEK expression plasmid (Addgene plasmid repository, plasmid number: 21208: W1), a plasmid expressing the wild type form of MEK. In parallel experiments, 3T3 cells were subject to three treatments along with control cells with no treatment, 1) Cells that were treated with MEK siRNA alone, 2) cells that were transiently transfected with both MEK siRNA and MEK expression plasmid (MEKp), 3) Cells that were transiently transfected with MEKp alone (Fig. 16). After 48hrs of treatment (see Materials and Methods for details), the total RNA from each of the treated cells along with control cells was isolated and the isolated RNA was subject to a Reverse Transcriptase-Polymerase

Chain Reaction (RT-PCR) procedure where, the total isolated RNA from each treatment and control cells was transcribed to form the corresponding cDNA by an RT reaction, then the cDNA was amplified by a PCR reaction using the specific 5' and 3' DNA primers. The amplified cDNA was then subject to agarose gel electrophoresis (see Materials and Methods for details). Glyceraldehyde-6-phosphate dehydrogenase (GAPDH) expression was studied as a control since it is a known housekeeping gene and is often stably and constitutively expressed at high levels in most tissues and cells (Barber et al. 2005; Zainuddin et al. 2010). For each experimental sample the 5'-3' primers for GAPDH and MEK were used in order to amplify the corresponding cDNA.

In Figure 16a lane 2 was loaded with control cell cDNA amplified with MEK primers while lane 3 was loaded with control cell cDNA amplified with GAPDH primers. Lanes 2 and 3 indicate that MEK cDNA and GAPDH cDNA were present in control cells. In lanes 4, 5 the amplified cDNA from cells treated with MEK siRNA alone was loaded. MEK cDNA (using MEK primers) cannot be seen (lane 4) since its synthesis was inhibited by the siRNA, while GAPDH cDNA (using GAPDH primers) can still be seen (lane 5) similar to that seen in the control lane 3. In lanes 6, 7, the amplified cDNA from cells transfected with only MEKp was loaded. Both MEK cDNA (using MEK primers) and GAPDH cDNA (using GAPDH primers) can be seen similar to that seen in the control lanes 2 and 3. Lanes 1 and 10 in figure 16a were loaded with a 1kb DNA ladder.

Expression at the protein level, of these RT-PCR results was examined next by immunoblotting (Fig. 16b, c). In parallel experiments, the cells were

subject to the same treatments described in the above section along with control cells, and DMSO carrier treated cells. The total cell lysates were isolated and immunoblotting was then performed with the lysates. Antibodies against tMEK (Fig. 16b) and against pMEK (Fig. 16c) were used to visualize the protein expression of tMEK and pMEK. Total MEK (Fig. 16b) was expressed from: a) Control cells that were not transfected; b) Cells that were transfected with both MEK siRNA and MEKp; c) Cells that were transfected with only MEKp. However, there was no expression of tMEK in the lane containing the lysate from cells transfected with only MEK siRNA compared to the expression in control cell lysates. This result was similar to the cDNA results in figure 16a. Similar to the protein expression results of tMEK, figure 16c indicates that pMEK was also expressed from: a) Control cells that were not transfected; b) Cells that were transfected with both MEK siRNA and MEKp; c) Cells that were transfected with only MEKp. However, there was no expression of pMEK in the lane containing the lysate from cells transfected with only MEK siRNA compared to the expression in control cell lysates.

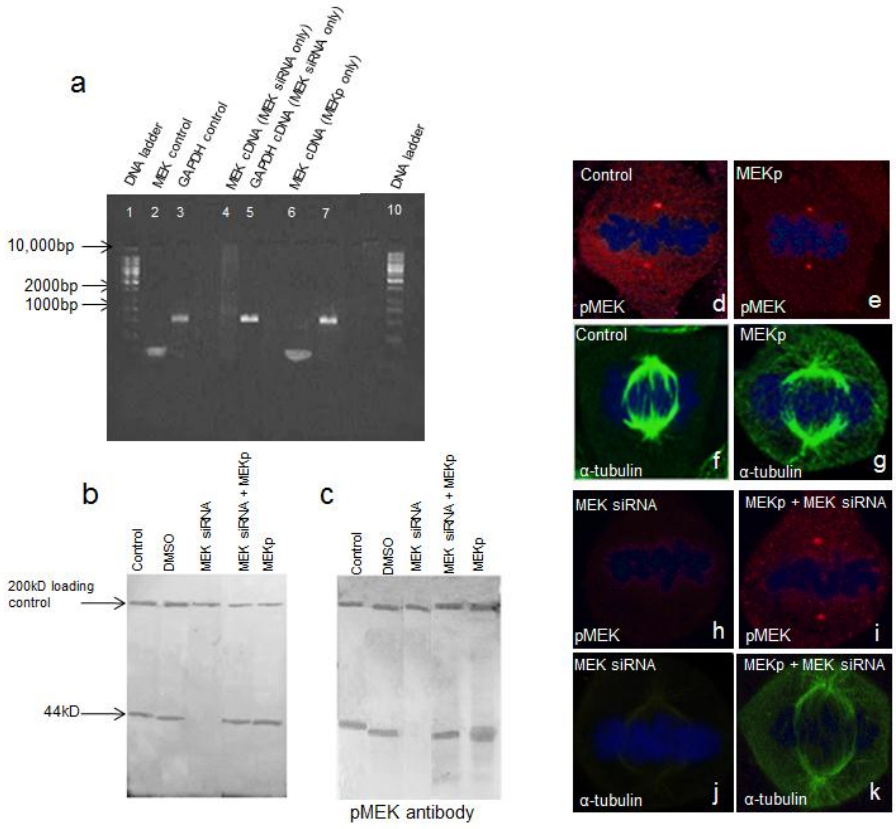

Figure 16. Confirmation of MEK siRNA specificity; Effect of MEK overexpression. (a) The PCR amplified cDNA was run on an agarose gel. The cDNA was processed by a reverse transcriptase reaction from cellular RNA. This RNA was isolated from cells treated with MEK siRNA alone, MEK plasmid alone (MEKp), a combination of MEK siRNA and MEK plasmid along with untreated control cells. For the PCR reaction, GAPDH primer set and MEK primer set were used. MEK cDNA can be visualized on the gel in MEKp treated cells, but not in MEK siRNA treated cells. (b) Western analysis of cell lysates from control cells, MEK siRNA treated cells, MEK siRNA and MEKp treated cells, and MEKp treated cells. An antibody to tMEK was used and tMEK protein bands can be detected in all the lanes except MEK siRNA treated cell lysate. (c) Western analysis of cell lysates from control cells, MEK siRNA treated cells, MEK siRNA and MEKp treated cells, and MEKp treated cells. An antibody to pMEK was used and pMEK protein bands can be detected in all the lanes except MEK siRNA treated cell lysate. Immunocytochemical analysis followed by confocal imaging was performed to study the effect of MEK overexpression on the enrichment of pMEK and α-tubulin. (d) The enrichment of pMEK in a control cell versus (e) MEKp treated cell at the centrosomes is quite similar. However, compared to (f) the enrichment of α-tubulin on the spindle in a control cell (g) the enrichment of α-tubulin in a MEKp treated cell seems to show an increase in astral microtubules. Immunocytochemical analysis followed by confocal imaging

was performed to study the effect of adding MEK siRNA along with MEKp on the enrichment of pMEK and α-tubulin. (h) The absence of pMEK in a MEK siRNA treated cell can be compared to (i) where there was enrichment of pMEK when MEKp was added together with MEK siRNA. (j) The reduction in intensity of green α-tubulin (part of the spindle microtubules) in MEK siRNA treated cell can be compared to (k) the spindle microtubules in a cell treated with both MEK siRNA and MEKp, where the spindle is similar to the spindle in a control cell.

The effects of overexpression of MEK on pMEK and α-tubulin were studied next at the immunocytochemical level. Cells were subjected to three types of treatments along with the untreated controls in separate experiments. The three types of treatments include, transfection of cells with MEKp, treatment of cells with MEK siRNA alone, treatment of cells with a combination of MEK siRNA and MEKp. These three types of cell populations along with controls were labeled with pMEK antibodies (red). The cells treated with MEKp alone showed the presence of pMEK (Fig. 16e) similar to the control cells (Fig. 16d). The MEK siRNA treated cells showed the absence of an enrichment of pMEK (Fig 16h), while the cells treated with both MEK siRNA and MEKp showed an enrichment of pMEK. The three types of cell populations along with controls were labeled next with α-tubulin antibodies (green). In MEKp treated cells the astral microtubules of the spindle are more pronounced (Fig. 16g) compared to those in the control cells (Fig. 16f). Compared to the MEK siRNA treated cell (Fig. 16j) where the spindle microtubules are highly reduced in intensity, in cells treated with both MEK siRNA and MEKp the spindle microtubules are almost similar to the untreated control microtubules.

Effects of MEK inhibition on the mitotic spindle

In order to assess the effects of inhibiting MEK on the mitotic spindle, cells were treated with MEK inhibitors in parallel experiments. An antibody against α-tubulin along with DRAQ5, was used to visualize the spindle microtubules and chromosomes in three stages of mitosis, namely metaphase, anaphase, and telophase. In figure 17a, the metaphase mitotic spindle of a control cell (α-tubulin, green) is shown. An intact spindle apparatus at this stage with intact microtubules enveloping the chromosomes (blue) from both spindle pole regions can be visualized. However, in cells treated with MEK siRNA (Fig. 17b) the metaphase spindle visualized by α-tubulin (green) indicates a reduction in brightness of microtubules compared to the control metaphase spindle in figure 17a. In cells treated with U0126, the metaphase spindle visualized by α-tubulin as green (Fig. 17c) also indicates a reduction in the brightness of microtubules compared to the control. In order to quantify this, the number of green pixels in the region of the spindle was quantified. One hundred cells were visualized at each stage of M-phase and a graphical representation of the spindle pixel intensity numbers at each M-phase stage is shown in figure 17j for controls and each treatment. All the pixel intensity numbers in figure 17j represent average pixel values of the entire spindle apparatus at each stage of the cell cycle. Statistical significance of these numbers was also calculated (see Materials and Methods section).

Anaphase stage in control cells visualized by α-tubulin (green) demonstrates intact microtubules (Fig. 17d) in a representative control cell. The

MEK siRNA treated cells indicate a reduction in pixel intensity (Fig. 17j) of microtubules visualized by α-tubulin antibody (green, Fig. 17e) compared to the control (Fig. 17d). Similarly in U0126 treated cells, the mitotic spindle in anaphase visualized by α-tubulin (green, Fig. 17f) indicates a reduction in the pixel intensity of microtubules (Fig. 17j), compared to the control cell (Fig. 17d).

Telophase stage in control cells (Fig. 17g) demonstrates that the microtubules are intact as visualized by α-tubulin (green) at the spindle apparatus region. However, in MEK siRNA treated cells (Fig. 17h), the pixel intensity of microtubules was reduced (Fig. 17j), visualized by α-tubulin (green) compared to the control cell in figure 17g. In the telophase stage of U0126 treated cells also (Fig. 17i) there was a reduction in the pixel intensity of microtubules (Fig. 17j) visualized by the α-tubulin antibody (green) compared to the control cell (Fig. 4g). In any of these three stages, the size of the spindle in MEK inhibitor treated cells did not change (data not shown).

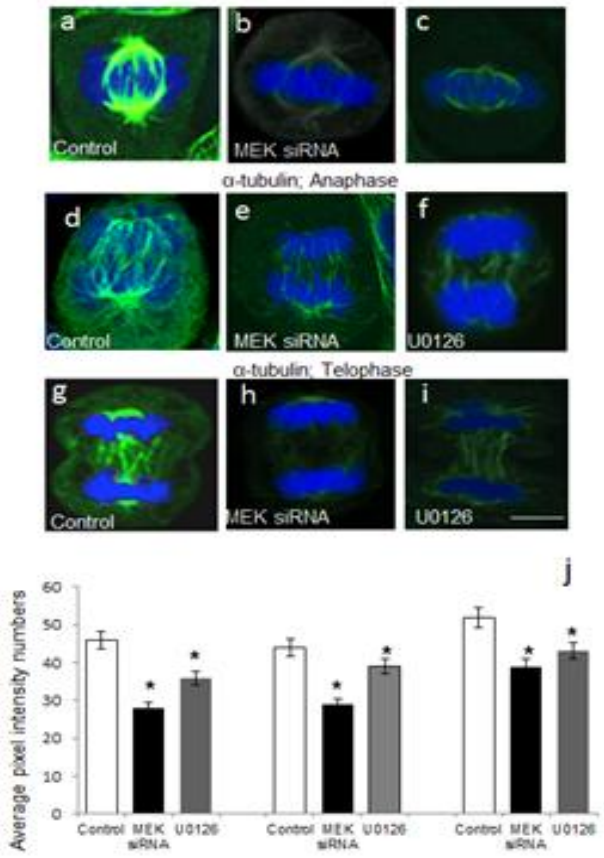

Figure 17: Effect of MEK inhibition on α-tubulin. (a) A control cell at metaphase showing an intact mitotic spindle. (b) A MEK siRNA treated cell indicating a reduction in the green pixel intensity of spindle microtubules at metaphase. (c) A U0126 treated cell indicating a reduction in the green pixels of spindle at metaphase. (d, e, f) A control cell, a cell treated with MEK siRNA, and a cell treated with U0126 respectively indicating a reduction in green pixel intensity of the spindle at anaphase. (g, h, i) Control cell versus MEK siRNA treated cell and U0126 treated cell respectively at telophase indicating a pixel intensity reduction in MEK inhibited cells. (j) The pixel intensity values for metaphase, anaphase and telophase are indicated in the histogram. The asterisks represent a significant difference from the control pixel intensity values. Experiments were performed in triplicate and statistical significance was calculated by a Student t-test and a probability of $p<0.05$ was considered as significant.

Effect of MEK inhibition on number of cells in cell division stages

Inhibition of MEK did not result in the disruption of the spindle though it did have the subtle effect of reducing the intensity of α-tubulin in spindle

microtubules. In order to test whether other subtle effects on mitosis occurred, progression through the cell cycle was assessed (Fig. 18). In parallel experiments, cells were treated with MEK siRNA and U0126 inhibitors along with the untreated control cells. The percent cell population in interphase and in each stage of M-phase including, pre-metaphase, metaphase, anaphase, telophase, and cytokinesis was examined by immunocytochemistry. The pre-metaphase stage encompassed all cells from early prophase through prometaphase. Spindle microtubules were identified by using antibodies against α-tubulin (green), while the chromosomes were identified with DRAQ5. The number of control cells examined were 4244 where, 1% cells were in pre-metaphase stages, 1.5% cells were in metaphase, 0.6% cells were in anaphase, 0.4% cells were in telophase and 0.5% cells were in the cytokinesis stage (Fig. 18a). The absolute numbers of cells for each stage of M-phase are indicated above the corresponding columns in figure 18a. A total of 4% cells were in the mitotic phase while 96% (4092 cells) were in interphase stages of the cell cycle indicated by the pie chart in figure 18a.

In MEK siRNA treated cells (Fig. 18b), 4172 cells were examined and the percent cells in each M-phase stage were significantly lower than the corresponding control cells. The absolute numbers of cells in each stage of M-phase are indicated above the corresponding columns in figure 18b. A total of 1.25% cells were present in the mitotic phase while 98.75% (4111) cells were present in interphase stages of the cell cycle (pie chart in figure 18b).

In U0126 treated cells also (Fig. 18c), 3975 cells were examined and the percent cells in each M-phase stage were significantly lower than the

corresponding control cells. The absolute numbers of cells in each stage of M-phase are indicated above the corresponding columns in figure 18c. A total of 1.5% cells were present in the mitotic phase while 98.5% (3916) cells were present in interphase stages of the cell cycle (pie chart in figure 18c). Statistical significance of these cell numbers from two treatments compared to the control cell numbers was calculated and a p-value of $p<0.05$ was considered significantly different in comparison to the control cells. The asterisks above the columns in the graph (Fig. 18b) indicate significant difference from the control cells.

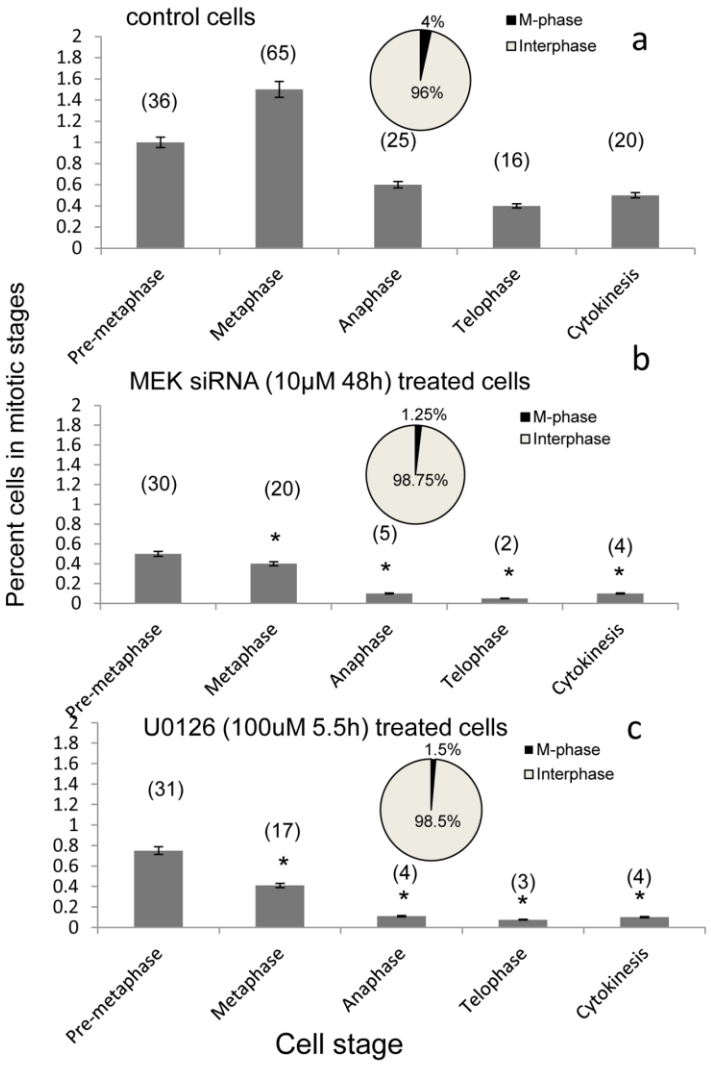

Figure 18: Cell numbers in mitotic stages after MEK inhibition. (a) The number of control cells in M-phase stages including, pre-metaphase (stages encompassing early prophase through prometaphase), metaphase, anaphase, telophase and cytokinesis are represented by a histogram. The pie chart inset in (a) indicates the percentage of cell in interphase versus M-phase. (b) The number of MEK siRNA treated cells in M-phase stages including, pre-metaphase (stages encompassing early prophase through prometaphase), metaphase, anaphase, telophase and cytokinesis are represented by a histogram. There is a significant reduction in the number of cells in M-phase stages compared to the control cell numbers which is indicated on the histogram by asterisks. (c) The number of U0126 treated cells in M-phase stages are represented by a histogram. A significant reduction in cell numbers compared to that of control cells is indicated by asterisks. Statistical significance was calculated by a Student t-test and a probability of $p<0.05$ was considered as significant. The pie chart insets in (b) and (c) represent the percent

cells in interphase versus M-phase and there is an increase in interphase cells when MEK is inhibited.

Effects of inhibition of ERK activation

To test if the ERK activation inhibitor has effects similar to that of the MEK inhibitors, on the number of cells in M-phase versus interphase, the percent cells in each of the M-phase stage were studied. The ERK inhibitor used was a peptide inhibitor that prevents activation of ERK by pMEK. The enrichment of active ERK (pERK) was detected in control cells by a pERK antibody (red, Fig. 19a), while in ERK inhibitor treated cells there is an absence of pERK (absence of red, Fig. 19b). Figure 19c shows a graphical representation of the percentage of cells in each of the mitotic stages studied. In this graph, control cell percentages (shown as white columns in figure 19a marked 'ctrl') were compared to the cells treated with the ERK1/2 peptide inhibitor (shown as black columns in figure 6c marked 'exp'). The number of cells counted for this study was 4200. Compared to the control cell percentages, a significantly lesser percentage of ERK inhibitor treated cells were present in the pre-metaphase and metaphase stages. Also, none of the ERK inhibitor treated cells were present in anaphase, telophase or cytokinesis compared to the control cells. The absolute numbers are indicated above the corresponding columns in figure 19c. A total of 99.6% cells were present in interphase stages while 0.4% cells were present in M-phase (pie-chart in Fig. 19c).

The protein expression patterns in control cells compared to ERK inhibited cells were examined next by immunoblotting using the antibodies

against the proteins indicated on the lanes (Fig. 19d). The untreated control cell lysates are indicated by "-" while ERK1/2 inhibitor treated cell lysates are indicated by "+" on the lanes in figure 19d. In the control cell lysate lane, the band for pERK can be visualized. In lane 3 of the blot, there is an absence of active pERK protein band, while lane 4 shows the presence of tERK (44kD and 42kD protein bands). The protein bands for pMEK and tMEK can be visualized in lanes 5 and 6 respectively in the inhibitor treated cell lysates. PhosphoPKCζ can be visualized in lane 7 and p(ser9)GSK3β can be visualized in lane 8 of figure 19d. Lane 9 shows the presence of α-tubulin. A comparison of the relative intensities of each protein band in the blot is shown as a histogram below the blot. From the histogram in figure 19d it can be seen that the amounts of pPKCζ, p(ser9)GSK3β, and α-tubulin proteins are significantly reduced in the ERK inhibitor added lysates compared to the control lysates.

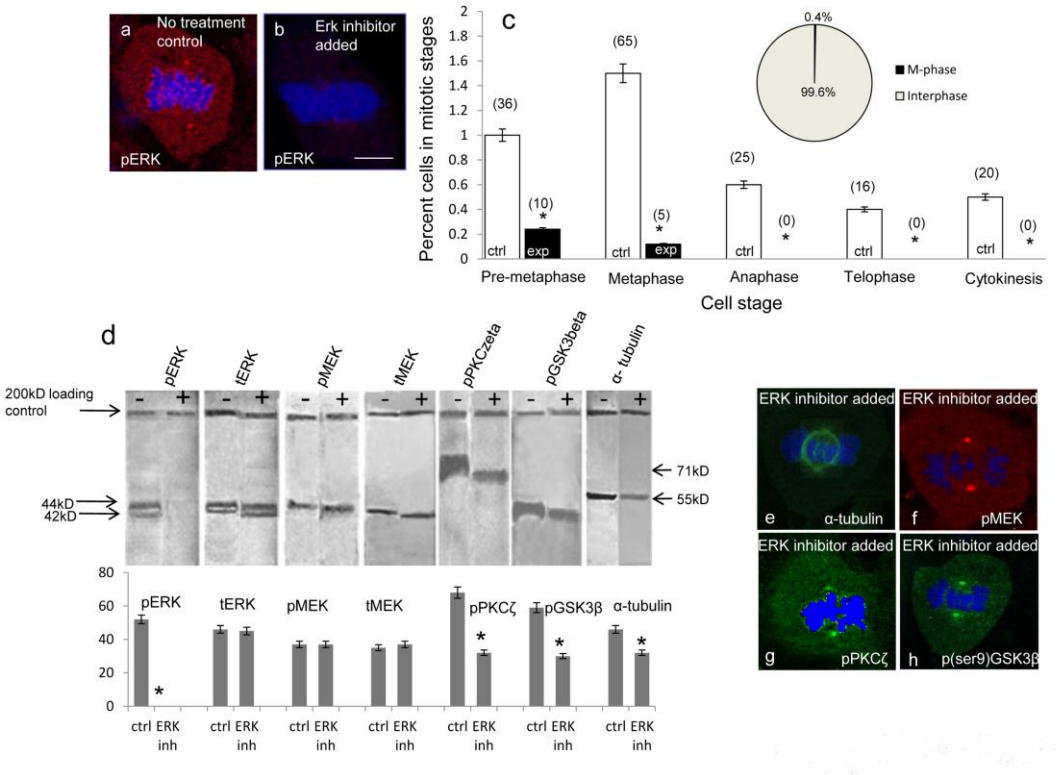

Figure 19: Effects of ERK activation peptide inhibitor. (a) pERK (red) exists at the centrosomes in control cells while (b) in ERK inhibitor treated cells there is an absence of pERK. (c) The number of control cells in M-phase (ctrl) versus the number of ERK inhibitor treated cells in M-phase (exp) are represented by a histogram. The M-phase stages that were counted include, pre-metaphase (stages encompassing early prophase through prometaphase), metaphase, anaphase, telophase and cytokinesis. In ERK inhibitor treated cells, no cells in anaphase, telophase and cytokinesis were identified. The pie chart inset in (c) indicates the percentage of cells in interphase versus M-phase. A significant reduction in cell numbers compared to that of control cells is indicated by asterisks. (d) Western analyses of control cell lysates (indicated by a '-'on the blot) versus ERK inhibitor treated cell lysates (indicated by a '+' on the blot). The antibodies used to detect corresponding proteins were, pERK, tERK, pMEK, tMEK, pPKCζ, p(ser9)GSK3β, and α-tubulin. The relative quantitation of these protein levels from the intensities of the protein bands is represented by a histogram below the western blots in (d). A significant reduction in band intensity compared to that of control cell lysates is indicated by asterisks. Statistical significance was calculated by a Student t-test and a probability of $p<0.05$ was considered as significant. (e) Cells treated with the ERK inhibitor were tested immunocytochemically for the enrichment of α-tubulin (green), (f) pMEK (red), (g) pPKCζ (green), and (h) p(ser9)GSK3β. It can be seen that these kinases are not absent at the centrosomes. All experiments were performed in triplicate.

ERK inhibited cells were labeled with an antibody against α-tubulin (green) visualized along the mitotic spindle in figure 19e. An antibody against pMEK (red) was visualized in the centrosome areas in figure 19f. An antibody against pPKCζ (green) was visualized in the centrosome areas in figure 19g. The enrichment of p(ser9)GSK3β (green) in the centrosome areas was visualized in figure 19h. The enrichment of pPKCζ and p(ser9)GSK3β at the centrosome was not absent in ERK inhibitor treated cells although the enrichment of α-tubulin along the mitotic spindle seems to have reduced compared to that in the MEK inhibited cells in figure 17.

Discussion

This study demonstrates that pMEK, pERK, pPKCζ, and p(ser9)GSK3β were all enriched at the centrosomes of the mitotic spindle in 3T3 cells. Also, pPKCζ and p(ser9)GSK3β each co-localized with pMEK and pERK at the centrosomes suggesting that these former two kinases may play an important role in mitotic spindle regulation. However inhibition of MEK by siRNA and by a chemical inhibitor indicated the following. 1) The enrichment of pPKCζ or p(ser9)GSK3β at the centrosomes was not inhibited, although there was a slight decrease in total cellular protein levels of pPKCζ and p(ser9)GSK3β. This suggested that these two kinases are not downstream targets of pMEK but may act either upstream of these kinases or alternatively may be in a separate pathway that engages in crosstalk with the MEK/ERK pathway. 2) There was a significant decrease in pixel intensity of the spindle microtubules when MEK was inhibited and the α-tubulin protein levels were also reduced. 3) The effect of MEK inhibition caused a slower progression of cells through M-phase compared to control cells. A peptide inhibitor that inhibited activation of ERK by pMEK was used and inhibition of pERK indicated the following. 1) The enrichment of pPKCζ or p(ser9)GSK3β at the centrosomes was not inhibited, as seen when MEK was inhibited. 2) There was a decrease in the α-tubulin protein levels and there was likely a decrease in the number of spindle microtubules. The number of spindle microtubules seemed to be further reduced than what was seen when MEK was inhibited. 3) In contrast to what was seen when MEK was inhibited,

inhibition of pERK caused an absence of cells in anaphase, telophase, and cytokinesis.

This study examined whether pMEK/pERK co-localized with pPKCζ and/or with p(ser9)GSK3β. Previously, the putative co-localization of these four kinases has not been examined in a single study. Separate studies have shown that pMEK, pERK, pPKCζ, and p(ser9)GSK3β are enriched at the centrosomes of the mitotic spindle (Lehrich and Forrest, 1994; Shapiro et al. 1998; Willard and Crouch, 2001; Etienne-Manneville and Hall, 2003; Wakefield et al. 2003; Jope and Johnson, 2004; Liu et al. 2006; Kalive et al. 2011; Collelo et al. 2012) but have not examined their interactions. Results from this study indicated that p(ser9)GSK3β and pPKCζ are possibly involved in maintaining an intact mitotic spindle independent of the MEK/ERK pathway in mouse 3T3 fibroblasts, although earlier studies have indicated that p(ser9)GSK3β can act downstream of the MAPK pathway in other cells and is involved in maintaining the dynamic instability of microtubules (Goold et al. 1995; Goold et al. 1999; Scales et al. 2009). PKCζ also has been implicated by other studies to be upstream of the MAPK pathway (Berra et al. 1995; Short et al. 2006). We speculated that these kinases may independently regulate specific components of the spindle since the absence of MEK/ERK activity and the presence of p(ser9)GSK3β and pPKCζ at the centrosomes resulted in a partially intact spindle. Interestingly, in this study when MEK was overexpressed the astral microtubules seemed to have increased which suggested that MEK may also be involved in regulation of astral microtubules. Studies have shown microtubule associated proteins (MAPs) to be

substrates of both ERK and GSK3β, and performed specific functions to regulate microtubules (Goold et al. 1995; Scales et al. 2009). Other MAPs including MAP-1, MAP-2, MAP-4 have been shown to be substrates of ERK1/2 (Lin et al. 1993; Seger and Krebbs, 1995; Zhang and Liu, 2002) that are involved in nucleation and stabilization of microtubules (Sanchez et al. 2000). In the current study, the reduction in pixel intensity at the spindle suggested that the spindle may have fewer microtubules, if so, this reduced spindle number may be one reason for slow M-phase progression of MEK/ERK inhibited cells. Alternatively, other studies have shown that inhibition of MEK/ERK inhibits the phosphorylation of downstream cyclin dependent kinases (cdks) which in turn slows the progression of cells through M-phase (Pumiglia and Decker, 1997; Willard and Crouch, 2001; Horne and Guadagno, 2003; Harding et al. 2003; Chambard et al. 2007).

Phospho(ser9)GSK3β has been shown to be involved in transport of centrosomal proteins to the centrosome by stabilizing the dynein complex, resulting in the regulation of a focused microtubule organization (Fumoto et al. 2006; Izumi et al. 2008). In addition, pPKCζ, has been shown to be important for microtubule-kinetochore attachment (Liu et al. 2006). In another study, ERK was shown to phosphorylate the kinetochore motor protein CENP-E on sites that regulate the interaction of centromere-binding protein E (CENP-E) with microtubules. ERK could play a role in mitotic progression by altering the ability of CENP-E to mediate the interactions between chromosomes and microtubules (Zecevic et al. 1998; Willard and Crouch, 2001; Chambard et al. 2007). As an extension to these earlier studies, this study indicated that ERK inhibition did

cause slower mitotic progression in 3T3 cells possibly due to a reduction in the number of spindle microtubules. Since MEK/ERK, p(ser9)GSK3β, and pPKCζ seemed to regulate different parts of the mitotic spindle, absence of MEK/ERK alone is necessary but not indispensable for 3T3 cells to maintain a spindle. A previous study showed abnormal spindles in the metaphase stage of U0126 treated cells (Guadagno and Horne, 2003). Additionally, the current study indicated a significant decrease in pixel intensity of the spindle microtubules in U0126 treated and MEK siRNA treated cells compared to control cells in metaphase, anaphase and telophase stages. Thus there was a reduction in total number of spindle microtubules in all these stages. Inhibition of MEK/ERK however, did not shorten or lengthen the microtubules in 3T3 cells as observed in the current study. The reduction in total cellular protein levels of α-tubulin in MEK/ERK inhibited cells as demonstrated in the current study is a further confirmation of reduction in the number of spindle microtubules.

MEK/ERK, PKCζ, and p(ser9)GSK3β are kinases that are bound to scaffold proteins (Morrison and Davis, 2003; Macara, 2004; Moscat et al. 2006; Sacks, 2006; Marks et al. 2009). Scaffold proteins are molecular sockets that bind several signal transducing proteins in such a way that the signaling interactions are facilitated and rendered more specific (Marks et al. 2009). These kinases seem to specifically regulate different elements of the spindle apparatus in 3T3 cells. The results from our study indicated that the MEK/ERK pathway may not have an important role in regulation of the centrosome in somatic cells, but it does have an important role in spindle microtubule regulation along with

p(ser9)GSK3β and pPKCζ. The kinases, MEK, PKCζ and GSK3β are probably not part of a single signaling pathway, but have overlapping functions in regard to preserving normal centrosomes and normal spindles. Phospho(ser9)GSK3β and PKCζ may be involved in regulating the centrosome which is the microtubule organizing center of somatic cells (Compton, 2000; Debec et al. 2010;Walczak et al. 2010), both these kinases being part of an independent pathway. Alternatively, pPKCζ could be upstream of the MEK/ERK pathway and also upstream to GSK3β in parallel to the MEK/ERK pathway, leading to the regulation of different elements of the mitotic spindle. These four kinases are important for normal cell division and inhibition of any one of these kinases can affect cell division dynamics.

Chapter 4

CONCLUDING THOUGHTS

Conclusions from Chapter 2

The results from the study in Chapter 2 match our predictions proposed earlier that, in mitotic cells: 1) there is significant co-localization and molecular proximity between pPKCζ and inactive GSK3β in the regions of the centrosome and, 2) inhibitors of pPKCζ may act through GSK3β to disrupt the proteins involved in maintaining spindle stability as well as the spindle structure itself. In addition, the data resulting from this study indicates that among the phospho PKC isoforms studied, pPKCζ is more likely to be involved in stability of microtubules in the centrosomal mitotic spindle apparatus during cell division in mouse cells.

A comparison can be made between the acentrosomal meiotic spindle in mouse eggs and the centrosomal mitotic spindle in mouse fibroblast cells. The similarities between these two types of spindle are: 1) Among the pPKC isoforms tested, pPKCζ and pPKCδ localize in the meiotic spindle poles and at the centrosome of the mitotic spindle; 2) pPKCζ and pPKCδ enrich in the kinetochore region of both meiotic spindle and mitotic spindle; 3) GSK3β is also enriched in the spindle pole region of the meiotic spindle as well as at the centrosome of the mitotic spindle; 4) Among the pPKC isoforms tested there is higher binding between pPKCζ and p(ser9)GSK3β in the meiotic spindle poles and at the centrosome of the mitotic spindle. Two notable differences exist between the centrosomal and acentrosomal spindles. First, in the mouse egg, pPKCζ is present as a ring at the end of each spindle pole whereas in somatic cells pPKCζ localizes

at the centrosome. Second, in meiotic cells, pPKCγ localizes at the spindle poles, whereas in mitotic cells pPKCγ is associated with the spindle microtubule region at the centrosomal end.

The many similarities between centrosomal and acentrosomal spindles suggest that although the assembly of these two spindles is different, the proteins/signals regulating spindle dynamics may be the same.

Conclusions from Chapter 3

The study in Chapter 3 demonstrates that pMEK, pERK, pPKCζ, and p(ser9)GSK3β are all enriched at the centrosomes of the mitotic spindle in 3T3 cells. If MEK/ERK, PKCζ, and GSK3β interact then we predicted that they would co-localize at the spindle during mitosis. Our results indicate that there is co-localization between pMEK/pERK and pPKCζ, and between pMEK/pERK and p(ser9)GSK3β supporting our prediction. We predicted that if MEK and ERK have sole control over the mitotic spindle then inactivation of either MEK or ERK may obliterate the spindle and progression through mitosis would be absent. This prediction was not supported in our study. Our final prediction was, if multiple signaling pathways are involved, then a modification or reduction in the spindle might be observed and also a reduction in the progression through mitosis. This final prediction was supported in our study.

The results from our study indicate that the MEK/ERK pathway may not have sole control in regulation of the centrosome in somatic cells, but that it does have an important role in spindle microtubule regulation along with

p(ser9)GSK3β and pPKCζ. The kinases, MEK, PKCζ and GSK3β are probably not part of a single signaling pathway, but have overlapping functions in regard to preserving normal centrosomes and normal spindles. Alternatively, pPKCζ could be upstream of the MEK/ERK pathway and also upstream to GSK3β in parallel to the MEK/ERK pathway, leading to the regulation of different elements of the mitotic spindle. The results from our studies suggest that these four kinases are important for normal cell division and inhibition of any one of these kinases can affect cell division dynamics.

The four kinases although not part of one signaling pathway, have specific roles to play in spindle regulation. Thus, the mitotic spindle itself may serve as a molecular scaffold where the kinases MEK/ERK, PKCζ, and p(ser9)GSK3β are bound and perform specific functions related to the regulation of the mitotic spindle. Molecular scaffolds are similar to sockets that bind several signal transducing proteins in such a way that the signaling interactions are facilitated and rendered more specific (Marks et al., 2009). For example, protein scaffolds bind to multiple components of the MAPK cascade, bringing them into close proximity and thereby facilitating efficient propagation of the signal. Kinase suppressor of Ras (KSR), IQGAP1, MEK partner-1 (MP-1), and β-arrestins are some of the scaffolds in the MAPK pathway that bind to MEK1/2 and ERK1/2 (Brown and Sacks, 2009). Par-6 and p62 are examples of scaffold proteins in cells that PKCζ binds to, in order to perform specific functions (Moscat et al. 2006).

A model pathway can be predicted from the results presented in Chapters 2 and 3 of the dissertation. The predicted model is indicated in figure 20 below.

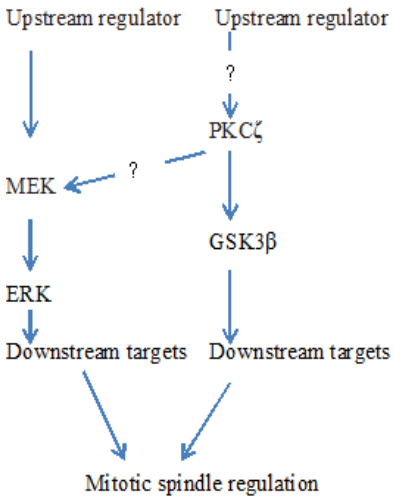

Figure 20: Predicted model from the results in Chapter 2 and Chapter 3.

In this predicted model, the upstream regulators of MEK and PKCζ that are involved in regulation of the mitotic spindle in 3T3 cells are not known. Also the downstream targets of ERK and GSK3β that are involved in mitotic spindle regulation of 3T3 cells are not known. This model can be used to suggest studies that can be conducted in future experiments.

Future studies

The function of each of the PKC isoforms in centrosome regulation should be investigated in the future. Since PKCδ is also found on the centrosome and binds p(ser9)GSK3β studies can be performed to determine if PKCδ is a 'backup'

kinase for PKCζ or if PKCδ has some other important role to play in mitotic spindle regulation. Studies can be performed to study upstream regulators of PKCζ and downstream effectors of GSK3β in 3T3 mouse fibroblast cells that are part of the pathway that regulates the mitotic spindle. This would identify the kinases that are involved in regulation of the spindle and are part of the same pathway.

In order to understand if PKCζ is upstream to the MAPK pathway, a peptide inhibitor against pPKCζ can be used and the cellular presence of pMEK and pERK can be investigated. If the pPKCζ inhibitor inhibits the presence of pMEK and pERK, pPKCζ can be further studied as an upstream regulator of pMEK and pERK. PKCs have been reported previously as upstream activators of the MEK/ERK pathway (Brändlin et al., 2002; Puente et al., 2006; Chang et al., 2008; Marks et al., 2009). In other studies the PKCζ isoform has been implicated to be an upstream activator of MEK (Berra et al. 1995; Short et al., 2006). Studies have shown microtubule associated proteins (MAPs) to be substrates of both ERK and GSK3β, and performed specific functions to regulate microtubules (Goold et al., 1995; Scales et al., 2009). In 3T3 cells it will be interesting to study if MAPs are downstream effectors of ERK and GSK3β.

The upstream regulator of PKCζ should be studied next in order to understand the complete pathway that regulates the mitotic spindle. Earlier studies have implicated Phosphoinositide-3-kinase (PI3K) as an upstream regulator of PKC (Populo et al. 2012; Lee et al. 2008). In other studies phosphoinositide dependent kinase-1 (PDK1) also has been implicated to be an

upstream regulator of PKC (Bayascas, 2010; Corbit et al. 2000). It will be interesting to investigate if PI3K and/or PDK1 are upstream regulators of PKCζ. Thus studying these aspects of the signaling pathways involving PKCζ, GSK3β, MEK and ERK discussed above may lead to interesting observations about the roles of these kinases in regulation of the mitotic spindle.

REFERENCES

Andersen SS, Ashford AJ, Tournebize R, Gavet O, Sobel A, Hyman AA, Karsenti E. 1997. Mitotic chromatin regulates phosphorylation of Stathmin/Op18. Nature. 389: 640–643.

Avazeri N, Courtot AM, Lefevre B. 2004. Regulation of spontaneous meiosis resumption in mouse oocytes by various conventional PKC isozymes depends on cellular compartmentalization. J Cell Sci 117:4969–4978.

Baluch DP, Capco DG. 2002. Cellular scaffolds in mammalian eggs. Front. Biosci. 7: 653–661.

Baluch DP, Capco DG. 2008. GSK3 beta mediates acentromeric spindle stabilization by activated PKC zeta. Dev. Biol. 317: 46–58.

Baluch DP, Koeneman BA, Hatch KR, McGaughey RW, Capco DG. 2004. PKC isotypes in post-activated and fertilized mouse eggs: association with the meiotic spindle. Dev. Biol. 274: 45–55.

Bayascas JR. 2010. PDK1: the major transducer of PI 3-kinase actions. Curr Top Microbiol Immunol. 346:9-29. Review

Berra E, Díaz-Meco MT, Lozano J, Frutos S, Municio MM, Sánchez P, Sanz L, Moscat J. 1995. Evidence for a role of MEK and MAPK during signal transduction by protein kinase C zeta. EMBO J. 14:6157-6163.

Brändlin I, Hübner S, Eiseler T, Martinez-Moya M, Horschinek A, Hausser A, Link G, Rupp S, Storz P, Pfizenmaier K, Johannes FJ. 2002. Protein kinase C (PKC) eta-mediated PKC mu activation modulates ERK and JNK signal pathways. J Biol Chem. 277:6490-6496.

Brinkley BR, Stubblefield E. 1966. The fine structure of the kinetochore of a mammalian cell in vitro. Chromosoma. 19:28-43.

Brunet S, Polanski Z, Verlhac MH, Kubiak JZ, Maro B. 1998. Bipolar meiotic spindle formation without chromatin. Curr Biol. 8:1231-1234.
Borysova MK, Cui Y, Snyder M, Guadagno TM. 2008. Knockdown of B-Raf impairs spindle formation and the mitotic checkpoint in human somatic cells. Cell Cycle. 7: 2894-2901.

Burbank KS, Mitchison TJ, Fisher DS. 2007. Slide-and-cluster models for spindle assembly.

Capco DG, Munoz DM, Gassmann CJ. 1987. A method for the analysis of the detergent-resistant cytoskeleton of cells within organs. Tissue Cell. 19: 607–616.

Caudron M, Bunt G, Bastiaens P, Karsenti E. 2005. Spatial coordination of spindle assembly by chromosome-mediated signaling gradients. Science. 309:1373-1376.

Chambard JC, Lefloch R, Pouysségur J, Lenormand P. 2007. ERK implication in cell cycle regulation. Biochim Biophys Acta. 8: 1299-1310.

Chang SJ, Tzeng CR, Lee YH, Tai CJ. 2008. Extracellular ATP activates the PLC/PKC/ERK signaling pathway through the P2Y2 purinergic receptor leading to the induction of early growth response 1 expression and the inhibition of viability in human endometrial stromal cells. Cell Signal. 20:1248-1255.

Chen D, Purohit A, Halilovic E, Doxsey SJ, Newton AC. 2004. Centrosomal anchoring of protein kinase C betaII by pericentrin controls microtubule organization, spindle function, and cytokinesis. J. Biol. Chem. 279: 4829–4839.

Colello D, Mathew S, Ward R, Pumiglia K, LaFlamme SE. 2012. Integrins regulate microtubule nucleating activity of centrosome through mitogen-activated protein kinase/extracellular signal-regulated kinase kinase/extracellular signal-regulated kinase (MEK/ERK) signaling. J Biol Chem. 287:2520-2530.

Compton D. A. 2000. Spindle assembly in animal cells. Annu. Rev. Biochem. 69: 95–114.

Cooke CA, Bazett-Jones DP, Earnshaw WC, Rattner JB. 1993. Mapping DNA within the mammalian kinetochore. J Cell Biol. 5:1083-91.
Corbit KC, Trakul N, Eves EM, Diaz B, Marshall M, Rosner MR. 2003. Activation of Raf-1 signaling by protein kinase C through a mechanism involving Raf kinase inhibitory protein. J Biol Chem. 278: 13061-13068.

Corbit KC, Soh JW, Yoshida K, Eves EM, Weinstein IB, Rosner MR. 2000. Different protein kinase C isoforms determine growth factor specificity in neuronal cells. Mol Cell Biol. 20 :5392-403.

Correas I, Díaz-Nido J, Avila J. 1992. Microtubule-associated protein tau is phosphorylated by protein kinase C on its tubulin binding domain. J. Biol. Chem. 267: 15721–15728.

Debec A, SullivanW, Bettencourt-Dias M. 2010. Centrioles: active players or passengers during mitosis. Cell Mol. Life Sci. 67: 2173–2194.

Denys A, Avazeri N, Lefevre B. 2007. The PKC pathway and in particular its beta1 isoform is clearly involved in meiotic arrest maintenance but poorly in FSH-induced meiosis resumption of the mouse cumulus cell enclosed oocyte. Mol Reprod Dev 74:1575–1580.

Doble BW, Woodgett JR. 2003. GSK-3: tricks of the trade for a multitasking kinase. J. Cell Sci. 116: 1175–1186.

Duncia JV, Santella JB 3rd, Higley CA, Pitts WJ, Wityak J, Frietze WE, Rankin FW, Sun JH, Earl RA, Tabaka AC, Teleha CA, Blom KF, Favata MF, Manos EJ, Daulerio AJ, Stradley DA, Horiuchi K, Copeland RA, Scherle PA, Trzaskos JM, Magolda RL, Trainor GL, Wexler RR, Hobbs FW, Olson R.E. 1998. MEK inhibitors: the chemistry and biological activity of U0126, its analogs, and cyclization products. Bioorg Med Chem Lett. 8: 2839-2844.

Durgan J, Cameron A J, Saurin AT, Hanrahan S, Totty N, Messing RO, Parker P J. 2008. The identification and characterization of novel PKC epsilon phosphorylation sites provide evidence for functional cross-talk within the PKC superfamily. Biochem. J. 411: 319–331.

Eng CH, Huckaba TM, Gundersen GG. 2006. The formin mDia regulates GSK3beta through novel PKCs to promote microtubule stabilization but not MTOC reorientation in migrating fibroblasts. Mol. Biol. Cell 17: 5004–5016.

Etienne-Manneville S, Hall A. 2003. Cdc42 regulates GSK-3β and adenomatous polyposis coli to control cell polarity. Nature 421: 753–756.

Favata MF, Horiuchi KY, Manos EJ, Daulerio AJ, Stradley DA, Feeser WS, Van Dyk DE, Pitts WJ, Earl RA, Hobbs F, Copeland RA, Magolda RL, Scherle PA, Trzaskos JM. 1998. Identification of a novel inhibitor of mitogen-activated protein kinase kinase. J Biol Chem. 273:18623-18632.

Frame S, Cohen P. 2001. GSK3 takes centre stage more than 20 years after its discovery. Biochem. J. 359: 1–16.

Fumoto K, Hoogenraad CC, Kikuchi A. 2006. GSK-3beta-regulated interaction of BICD with dynein is involved in microtubule anchorage at centrosome. EMBO J. 25: 5670-5682.

Gangeswaran R, Jones KT. 1997. Unique protein kinase C profile in mouse oocytes: lack of calcium-dependent conventional isoforms suggested by rtPCR and Western blotting. FEBS Lett. 412: 309–312.

Goold R. G, Gordon-Weeks PR. 2001. Microtubule-associated protein 1B phosphorylation by glycogen synthase kinase 3beta is induced during PC12 cell differentiation. J. Cell Sci. 114: 4273–4284.

Goold RG, Gordon-Weeks PR. 2004. Glycogen synthase kinase 3beta and the regulation of axon growth. Biochem. Soc. Trans. 32: 809–811.

Goold RG, Owen R, Gordon-Weeks PR. 1999. Glycogen synthase kinase3β phosphorylation of microtubule-associated protein 1B regulates the stability of microtubules in growth cones. J. Cell Sci. 112: 3373–3384.

Goshima G, Nédélec F, Vale RD. 2005. Mechanisms for focusing mitotic spindle poles by minus end-directed motor proteins. J Cell Biol. 171:229-240.
Guadagno TM, Ferrell JE Jr. 1998. Requirement for MAPK activation for normal mitotic progression in Xenopus egg extracts. Science. 282: 1312-1315.

Harding A, Giles N, Burgess A, Hancock JF, Gabrielli BG. 2003. Mechanism of mitosis-specific activation of MEK1. J Biol Chem. 278: 16747-16754.

Hayne C, Tzivion G, Luo, Z. 2000. Raf-1/MEK/MAPK pathway is necessary for the G2/M transition induced by nocodazole. J. Biol. Chem. 275: 31876–31882.

Heald R, Tournebize R, Blank T, Sandaltzopoulos R, Becker P, Hyman A, Karsenti E. 1996. Self-organization of microtubules into bipolar spindles around artificial chromosomes in Xenopus egg extracts. Nature. 382:420-425.

Hernandez AI, Blace N, Crary JF, Serrano PA, Leitges M, Libien JM, Weinstein G, Tcherapanov A, Sacktor TC. 2003. Protein kinase M zeta synthesis from a brain mRNA encoding an independent protein kinase C zeta catalytic domain. Implications for the molecular mechanism of memory. J. Biol. Chem. 278: 40305–40316.

Habermann, Lange. 2012. New insights into subcomplex assembly and modifications of centrosomal proteins. Cell Div. 7:17. [Epub].

Holland AJ, Cleveland DW. 2009. Boveri revisited: chromosomal instability, aneuploidy and tumorigenesis. Nat Rev Mol Cell Biol. 10:478-487.

Holy TE, Leibler S. 1994. Dynamic instability of microtubules as an efficient way to search in space. Proc. Natl. Acad. Sci. 91:5682–5685.

Huang B, Huffaker TC. 2006. Dynamic microtubules are essential for efficient chromosome capture and biorientation in S. cerevisiae. J. Cell Biol. 175: 17–23.

Izumi N, Fumoto K, Izumi S, Kikuchi A. 2008. GSK-3beta regulates proper mitotic spindle formation in cooperation with a component of the gamma-tubulin ring complex, GCP5. J Biol Chem. 2008. 283: 12981-12991.

Jackman J, O'Connor PM. 1998. Methods for synchronizing cells at specific stages of the cell cycle. Curr. Prot. Cell Biol. 8.3.1–8.3.20.

Jaken S, Parker PJ. 2000. Protein kinase C binding partners. Bioessays 22: 245–254.

Jope RS, Johnson GV. 2004. The glamour and gloom of glycogen synthase kinase-3. Trends. Biochem. Sci. 29: 95–102.

Kalive M, Faust JJ, Koeneman BA, Capco DG. 2009. Involvement of the PKC family in regulation of early development. Mol. Reprod.Dev. 77: 95–104.

Kalive M, Baluch DP, Capco DG. 2012. Involvement of PKCζ and GSK3β in the stability of the metaphase spindle. In Vitro Cell Dev Biol Anim. 2:97-111.

Karsenti E, Vernos I. 2001. The mitotic spindle: a self-made machine. Science 294: 543–547. Kholodenko BN. 2006. Cell-signalling dynamics in time and space. Nat Rev Mol Cell Biol. 3:165-176.

Kiley SC, Parker PJ. 1995. Differential localization of protein kinase C isozymes in U937 cells: evidence for distinct isozyme functions during monocyte differentiation. J. Cell Sci. 108: 1003–1016.

Kiley SC, Parker PJ. 1997. Defective microtubule reorganization in phorbol ester-resistant U937 variants: reconstitution of the normal cell phenotype with nocodazole treatment. Cell Growth Differ. 8:231–242.

Kim M, Datta A, Brakeman P, Yu W, Mostov KE. 2007. Polarity proteins PAR6 and aPKC regulate cell death through GSK-3beta in 3D epithelial morphogenesis. J. Cell Sci. 120: 2309–2317.

Koeneman B, Capco DG. 2004. Cell signaling. In: Meyers R. A. (ed) Encyclopedia of molecular cell biology and molecular medicine. Wiley, VCH vol 2, pp 463–486.

Krishnamurthy K, Wang G, Silva J, Condie BG, Bieberich E. 2007. Ceramide regulates atypical PKCζ/λ-mediated cell polarity in primitive ectoderm cells. J. Biol. Chem. 282: 3379–3390.

Krotova K, Hanbo H, Shen-Ling X, Leonid B, Jawaharlal MP, Edward RB, Sergey Z. 2006. Peptides modified by myristoylation activate eNOS in endothelial cells through Akt phosphorylation. Br. J. Pharmacol. 148: 732–740.

Laemmli UK. 1970. Cleavage of structural proteins during the assembly of the head of bacteriophage T4. Nature 227: 680–685.

Lehrich RW, Forrest Jr. JN. 1994. Protein kinase C zeta is associated with the mitotic apparatus in primary cell cultures of the shark rectal gland. J. Biol. Chem. 269: 32446–32450.

Lee SH, Lee MY, Lee JH, Han HJ. 2008. A potential mechanism for short time exposure to hypoxia-induced DNA synthesis in primary cultured chicken hepatocytes: Correlation between Ca(2+)/PKC/MAPKs and PI3K/Akt/mTOR. J Cell Biochem. 104:1598-611.

Lin LL, Wartmann M, Lin AY, Knopf JL, Seth A, Davis RJ. 1993. cPLA2 is phosphorylated and activated by MAP kinase. Cell. 72: 269-278.

Liu SJ, Zhang AH, Li HL, Wang Q, Deng HM, Netzer WJ, Xu H, Wang JZ. 2003. Overactivation of glycogen synthase kinase-3 by inhibition of phosphoinositol-3 kinase and protein kinase C leads to hyperphosphorylation of Tau and impairment of spatial memory. J. Neurochem. 87: 1333–1344.

Liu XF, Xie X, Miki T. 2006. Inhibition of protein kinase C zeta blocks the attachment of stable microtubules to kinetochores leading to abnormal chromosome alignment. Cell. Signal. 18: 2314–2323.

Lovestone S, Hartley CL, Pearce J, Anderton BH. 1996. Phosphorylation of tau by glycogen synthase kinase-3 beta in intact mammalian cells: the effects on the organization and stability of microtubules. Neuroscience. 73:1145-1157.
Luria A, Tennenbaum T, Sun QY, Rubinstein S, Breitbart H. 2000. Differential localization of conventional protein kinase C isoforms during mouse oocyte development. Biol Reprod 62:1564–1570.

Ma W, Koch JA, Viveiros MM. 2008. Protein kinase C delta (PKCdelta) interacts with microtubule organizing center (MTOC)-associated proteins and participates in meiotic spindle organization. Dev Biol 320:414–425.

Macara IG. 2004. Parsing the polarity code. Nat Rev Mol Cell Biol.5: 220-231.
Maiato H, Rieder CL, Khodjakov A. 2004. Kinetochore-driven formation of kinetochore fibers contributes to spindle assembly during animal mitosis. J Cell Biol. 167:831-40.

Marks F, Klingmuller U, Muller-Decker K. 2009. Cellular signal processing: An introduction to the molecular mechanisms of signal transduction. Garland Science, Taylor and Francis group, LLC., NY USA. 31.31. McIntosh, J., and Landis, S.C. 1971. The distribution of spindle microtubules during mitosis in cultured human cells. J. Cell. Biol. 49: 468–497.

Meier M, Menne J, Haller H. 2009. Targeting the protein kinase C family in the diabetic kidney: Lessons from analysis of mutant mice. Diabetologia 52:765–775.

McEwen BF, Arena JT, Frank J, Rieder CL. 1993. Structure of the colcemid-treated PtK1 kinetochore outer plate as determined by high voltage electron microscopic tomography. J Cell Biol. 120:301-312.

Morrison DK, Davis RJ. 2003. Regulation of MAP kinase signaling modules by scaffold proteins in mammals. Annu Rev Cell Dev Biol. 19: 91-118.

Moscat J, Diaz-Meco MT, Wooten MW. 2006. Signal integration and diversification through the p62 scaffold protein. Trends Biochem Sci. 32: 95-100.

Musacchio A, Salmon ED. 2007. The spindle-assembly checkpoint in space and time. Nat Rev Mol Cell Biol. 8:379-93.

Na J, Zernicka-Goetz M. 2006. Asymmetric positioning and organization of the meiotic spindle of mouse oocytes requires CDC42 function. Curr Biol.16:1249–1254.

Nigg E. 2001. Mitotic kinases as regulators of cell division and its checkpoints. Nature reviews. 2: 21-32.

O'Connell CB, Khodjakov AL. 2007. Cooperative mechanisms of mitotic spindle formation. J. Cell Sci. 120: 1717–1722.

Orton R, Sturm OE, Vyshemirsky V, Calder M, Gilbert DR, Kolch W. 2005. Computational modelling of the receptor-tyrosine-kinase-activated MAPK pathway. Biochem. J. 392: 249–261.

Paoletti A, Bornens M. 1997. Organisation and functional regulation of the centrosome in animal cells. Prog Cell Cycle Res. 3:285-299.

Parkinson SJ, Le Good JA, Whelan RD, Whitehead P, Parker PJ. 2004. Identification of PKCζII: an endogenous inhibitor of cell polarity. EMBO J. 23: 77–88.

Passalacqua M, Patrone M, Sparatore B, Melloni E, Pontremoli S. 1999. Protein kinase C-theta is specifically localized on centrosomes and kinetochores in mitotic cells. Biochem. J. 337: 113–118.

Pauken CM, Capco DG. 2000. The expression and stage-specific localization of protein kinase C isotypes during mouse preimplantation development. Dev. Biol. 223: 411–421.

Pópulo H, Lopes JM, Soares P. The mTOR Signalling Pathway in Human Cancer. 2012. Int J Mol Sci. 13:1886-918. Epub 2012 Feb 10.

Przewloka MR, Glover DM. 2009. The kinetochore and the centromere: a working long distance relationship. Annu. Rev. Genet. 43: 439–465.

Puente LG, He JS, Ostergaard HL. 2006. A novel PKC regulates ERK activation and degranulation of cytotoxic T lymphocytes: Plasticity in PKC regulation of ERK. Eur J Immunol. 4: 1009-1018.

Pumiglia KM, Decker SJ. 1997. Cell cycle arrest mediated by the MEK/mitogen-activated protein kinase pathway. Proc Natl Acad Sci. 94: 448-452.

Quan HM, Fan HY, Meng XQ, Huo LJ, Chen DY, Schatten H, Yang PM, Sun QY. 2003. Effects of PKC activation on the meiotic maturation, fertilization and early embryonic development of mouse oocytes. Zygote 11:329–337.

Rajagopalan H, Lengauer C. 2004. Aneuploidy and cancer. Nature. 432:338-41.

Rao CV, Yamada HY, Yao Y, Dai W. 2009. Enhanced genomic instabilities caused by deregulated microtubule dynamics and chromosome segregation: a perspective from genetic studies in mice. Carcinogenesis. 2009. 30:1469-74.

Raz T, Eliyahu E, Yesodi V, Shalgi R. 1998. Profile of protein kinase C isozymes and their possible role in mammalian egg activation. FEBS Lett. 431: 415–418.

Ricke RM, van Deursen JM. 2011. Correction of microtubule-kinetochore attachment errors: mechanisms and role in tumor suppression. Semin Cell Dev Biol. 22:559-65.

Ris H, Witt PL. 1981. Structure of the mammalian kinetochore. Chromosoma. 82:153-70.

Roberts EC, Shapiro PS, Nahreini TS, Pages G, Pouyssegur J, Ahn NG. 2002. Mol. Cell. Biol. 22: 7226–7241.

Robinson D, Beattie P, Sherwin T, Gull K. 1991. Microtubules, tubulin, and microtubule-associated proteins of trypanosomes. Methods Enzymol. 196: 285–299.

Roffey J, Rosse C, Linch M, Hibbert A, McDonald NQ, Parker PJ. 2009. Protein kinase C interventions: the state of play. Curr. Opin.Cell Biol. 21: 268–279.

Rosse C, Linch M, Kermorgrant S, Cameron AJ, Boeckeler K, Parker PJ. 2010. PKC and the control of localized signal dynamics. Nat. Rev. Mol. Cell Biol. 11: 103–112.

Rozengurt E. 2007. Mitogenic Signaling Pathways Induced by G Protein-Coupled Receptors. J. Cell. Physiol. 213: 589–602.

Sacks DB. 2006. The role of scaffold proteins in MEK/ERK signalling. Biochem Soc Trans. 34: 833-6.

Saffery R, Irvine DV, Griffiths B, Kalitsis P, Choo KH. 2000. Components of the human spindle checkpoint control mechanism localize specifically to the active centromere on dicentric chromosomes. Hum Genet. 107: 376-384.

Sánchez C, Díaz-Nido J, Avila J. 2000. Phosphorylation of microtubule-associated protein 2 (MAP2) and its relevance for the regulation of the neuronal cytoskeleton function. Prog Neurobiol. 2000. 61: 133-168.

Scales TM, Lin S, Kraus M, Goold RG, Gordon-Weeks PR. 2009. Nonprimed and DYRK1A-primed GSK3 beta-phosphorylation sites on MAP1B regulate microtubule dynamics in growing axons. J Cell Sci. 122: 2424-2435.

Schmid-Alliana A, Menou L, Manié S, Schmid-Antomarchi H, Millet MA, Giuriato S, Ferrua, Rossi B. 1998. Microtubule integrity regulates src-like and extracellular signal-regulated kinase activities in human pro-monocytic cells. Importance for interleukin-1 production. J Biol Chem. 273: 3394-3400.

Schmidt S, Essmann F, Cirtea IC, Kuck F, Thakur HC, Singh M, Kletke A, Jänicke RU, Wiek C, Hanenberg H, Ahmadian MR, Schulze-Osthoff K, Nürnberg B, Piekorz RP. 2010. The centrosome and mitotic spindle apparatus in cancer and senescence. Cell Cycle. 9:4469-4473.

Schonwasser D, Marais RM, Marshall CJ. 1998. Activation of the Mitogen-activated protein kinase/extracellular signal-regulated kinase pathway by conventional, novel and atypical protein kinase C isotypes. Mol Cell Biol. 18:790-798.

Seger R, Krebs EG. 1995. The MAPK signaling cascade. FASEB J. 9: 726-35.

Shapiro PS, Vaisberg E, Hunt AJ, Tolwinski NS, Whalen AM, McIntosh JR, Ahn NG. 1998. Activation of the MKK/ERK pathway during somatic cell mitosis. J. Cell Biol. 142, 1533–1545.

Shaul YD, Seger R. 2007. The MEK/ERK cascade: from signaling specificity to diverse functions. Biochim Biophys Acta. 1773: 1213-26.

Short MD, Fox SM, Lam CF, Stenmark KR, Das M. 2006. Protein kinase Czeta attenuates hypoxia-induced proliferation of fibroblasts by regulating MAP kinase phosphatase-1 expression. Mol Biol Cell. 4: 1995-2008.

Steinberg SF. 2008. Structural basis of protein kinase C isoform function. Physiol. Rev. 88: 1341–1378.

Szollosi D, Calarco P, Donahue RP. 1972. Absence of centrioles in the first and second meiotic spindles of mouse oocytes. J Cell Sci. 11:521-41.

Takahashi M, Mukai H, Oishi K, Isagawa T, Ono Y. 2000. Association of immature hypophosphorylated protein kinase C epsilon with an anchoring protein CG-NAP. J. Biol. Chem. 275: 34592–34596.

Towbin H, Staehelin T, Gordon J. 1979. Electrophoretic transfer of proteins from polyacrylamide gels to nitrocellulose sheets: procedure and some applications. Biotechnology 24: 145–149.

Trivedi N, Marsh P, Goold RG, Wood-Kaczmar A, Gordon-Weeks PR. 2005. Glycogen synthase kinase-3beta phosphorylation of MAP1B at Ser1260 and Thr1265 is spatially restricted to growing axons. J.Cell Sci. 118: 993–1005.

Tulu US, Fagerstrom C, Ferenz NP, Wadsworth P. 2006. Molecular requirements for kinetochore-associated microtubule formation in mammalian cells. Curr Biol. 16:536-41.

Utton MA, Vandecandelaere A, Wagner U, Reynolds CH, Gibb GM, Miller CC, Bayley PM, Anderton BH. 1997. Phosphorylation of tau by glycogen synthase kinase 3beta affects the ability of tau to promote microtubule self-assembly. Biochem J. 323:741-747.

Vaughan KT. 2005. Microtubule plus ends, motors, and traffic of Golgi membranes. Biochim. Biophys. Acta 1744: 316–324.

Vernos I, Karsenti E. 1995. Chromosomes take the lead in spindle assembly. Trends Cell Biol. 5: 297–301.

Viveiros MM, Hirao Y, Eppig JJ. 2001. Evidence that protein kinase C (PKC) participates in the meiosis I to meiosis II transition in mouse oocytes. Dev. Biol. 235: 330–342.

Viveiros MM, O'Brien M, Wigglesworth K, Eppig JJ. 2003. Characterization of protein kinase C-delta in mouse oocytes throughout meiotic maturation and following egg activation. Biol. Reprod. 69: 1494–1499.

Volkov Y, Long A, Kelleher D. 1998. Inside the crawling T cell: leukocyte function-associated antigen-1 cross-linking is associated with microtubule-directed translocation of protein kinase C isoenzymes beta(I) and delta. J. Immunol. 161: 6487–6495.

Wagner U, Utton M, Gallo JM, Miller CC. 1996. Cellular phosphorylation of tau by GSK-3 beta influences tau binding to microtubules and microtubule organisation. J Cell Sci. 109:1537-1543.

Wakefield JG, Stephens DJ, Tavare JM. 2002. A role for glycogen synthase kinase-3 in mitotic spindle dynamics and chromosome alignment. J. Cell Sci. 116: 673–646.

Walsh S, Margolis SS, Kornbluth S. 2003. Phosphorylation of the cyclin b1 cytoplasmic retention sequence by mitogen-activated protein kinase and Plx. Mol Cancer Res. 4: 280-289.

Walczak CE, Heald R. 2008. Mechanisms of Mitotic Spindle Assembly and Function. Int. Rev. Cyt. 265: 111–158.

Walczak CE, Cai S, Khodjakov A. 2010. Mechanisms of chromosome behavior during mitosis. Nat. Rev. Mol. Cell Biol. 11: 91–102.

Wilding M, Wright EM, Patel R, Ellis-Davies G, Whitaker M. 1996. Local perinuclear calcium signals associated with mitosis-entry in early sea urchin embryos. J Cell Biol 135:191–199.

Willard FS, Crouch MF. 2001. MEK, ERK, and p90RSK are present on mitotic tubulin in Swiss 3T3 cells: a role for the MAP kinase pathway in regulating mitotic exit. Cell Signal. 9:653-664.

Wright JH, Munar E, Jameson DR, Andreassen PR, Margolis RL, Seger R, Krebs EG. 1999. Mitogen-activated protein kinase kinase activity is required for the G(2)/M transition of the cell cycle in mammalian fibroblasts. Proc. Natl. Acad. Sci. 96: 11335–11340.

Yung Y, Dolginov Y, Yao Z, Rubinfeld H, Michael D, Hanoch T, Roubini E, Lando Z, Zharhary D, Seger, R. 1997. Detection of ERK activation by a novel monoclonal antibody. FEBS Lett. 408: 292–296.

Yoshimura T, Kawano Y, Arimura N, Kawabata S, Kikuchi A, Kaibuchi K. 2005. GSK-3beta regulates phosphorylation of CRMP-2 and neuronal polarity. Cell 120: 137–149.

Zecevic M, Catling AD, Eblen ST, Renzi L, Hittle JC, Yen TJ, Gorbsky GJ, Weber MJ. 1998. Active MAP kinase in mitosis: localization at kinetochores and association with the motor protein CENP-E. J. Cell Biol. 142, 1547–1558.

Zhang D, Nicklas RB. 1995. The impact of chromosomes and centrosomes on spindle assembly as observed in living cells. J Cell Biol. 5:1287-1300.

Zhang W, Liu HT. 2002. MAPK signal pathways in the regulation of cell proliferation in mammalian cells. Cell Res. 1: 9-18.

Zhou FQ, Snider WD. 2005. GSK-3β and microtubule assembly in axons. Science 308: 211–214.

Zimmermann T, Rietdorf J, Girod A, Georget V, Pepperkok R. 2002. Spectral imaging and linear un-mixing enables improved FRET efficiency with a novel GFP2-YFP FRET pair. FEBS Lett. 531: 245–249.

111

111

111

111